Phytomedicine 126 (2024) 155267

Contents lists available at ScienceDirect

Phytomedicine

journal homepage: www.elsevier.com/locate/phymed

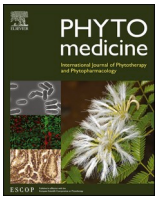

Original Article

Cytotoxicity of dioncophylline A and related naphthylisoquinolines in leukemia cells, mediated by NF-κB inhibition, angiogenesis suppression, G2/M cell cycle arrest, and autophagy induction

Rümeysa Yücer [a], Shaimaa Fayez [b,c], Doris Feineis [b], Sabine M. Klauck [d], Letian Shan [e], Gerhard Bringmann [b], Thomas Efferth [a], Mona Dawood [a,*]

[a] Department of Pharmaceutical Biology, Institute of Pharmaceutical and Biomedical Sciences, Johannes Gutenberg University, Staudinger Weg 5, Mainz 55128, Germany
[b] Institute of Organic Chemistry, University of Würzburg, Am Hubland, Würzburg 97074, Germany
[c] Home address: Department of Pharmacognosy, Faculty of Pharmacy, Ain-Shams University, Cairo, Egypt
[d] Division of Cancer Genome Research, German Cancer Research Center (DKFZ) Heidelberg, National Center for Tumor Diseases (NCT), NCT Heidelberg, a partnership between DKFZ and University Hospital Heidelberg, Germany
[e] The First Affiliated Hospital, Zhejiang Chinese Medical University, Hangzhou 310053, China

ARTICLE INFO

Keywords:
Cancer
Dioncophyllaceae
Drug development
Phytochemistry
Transcription factors
Zebrafish

ABSTRACT

Background: Inhibition of NF-κB activity represents a strategy to treat acute myeloid leukemia, one of the most lethal leukemia types. Naphthylisoquinolines (NIQs) are cytotoxic alkaloids from lianas of the families Ancistrocladaceae and Dioncophyllaceae, which are indigenous to tropical rainforests.

Purpose: Uncovering therapeutic possibilities and underlying molecular mechanisms of dioncophylline A and its derivatives towards NF-κB related cellular processes.

Methods: Resazurin-based cell viability assay was performed for dioncophylline A and three derivatives on wild-type CCRF-CEM and multidrug-resistant CEM/ADR5000 cells. Transcriptome analysis was executed to discover cellular functions and molecular networks associated with dioncophylline A treatment. Expression changes obtained by mRNA microarray hybridization were confirmed using qRT-PCR. Molecular docking was applied to predict the affinity of the NIQs with NF-κB. To validate the *in silico* approach, NF-κB reporter assays were conducted on HEK-Blue™ Null1 cells. Cell death mechanisms and cell cycle arrest were studied using flow cytometry. The potential activity on angiogenesis was evaluated with the endothelial cell tube formation assay on HUVECs using fluorescence microscopy. Intracellular NF-κB location in HEK-Blue™ Null1 cells was visualized with immunofluorescence. Finally, the anti-tumor activity of dioncophylline A was studied by a xenograft zebrafish model *in vivo*.

Results: Our study demonstrated that dioncophylline A and its derivatives exerted potent cytotoxicity on leukemia cells. Using Ingenuity Pathway Analysis, we identified the NF-κB network as the top network, and docking experiments predicted dioncophylline A and two of its derivatives sharing the same binding pocket with the positive control compound, triptolide. Dioncophylline A showed the best inhibitory activity in NF-κB reporter assays compared to its derivatives, caused autophagy rather than apoptosis, and induced G2/M arrest. It also prevented NF-κB translocation from the cytoplasm to the nucleus. Tube formation as an angiogenesis marker was significantly suppressed by dioncophylline A treatment. Finally, the remarkable anti-tumor activity of dioncophylline A was proven in zebrafish *in vivo*.

Conclusion: Taken together, we report for the first time the molecular mechanism behind the cytotoxic effect of dioncophylline A on leukemia cells. Dioncophylline A showed strong cytotoxic activity, inhibited NF-κB translocation, significantly affected the NF-κB *in silico* and *in vitro*, subdued tube formation, induced autophagy, and

Abbreviations: DDIT4L, DNA-damage-inducible transcript 4 like; ETV5, ETS variant transcription factor 5; HUVECs, human umbilical vein endothelial cells; ID1, inhibitor of DNA binding 1; IκB, inhibitory proteins; IPA, Ingenuity Pathway Analysis; LST1, leukocyte specific transcript 1; NF-κB, nuclear factor kappa B; NIQs, Naphthylisoquinolines; PBS, phosphate-buffered saline; SLC32A1, solute carrier family 32 member 1.

* Corresponding author.
E-mail address: modawood@uni-mainz.de (M. Dawood).

https://doi.org/10.1016/j.phymed.2023.155267
Received 28 August 2023; Received in revised form 22 November 2023; Accepted 7 December 2023
Available online 8 December 2023
0944-7113/© 2023 The Author(s). Published by Elsevier GmbH. This is an open access article under the CC BY license (http://creativecommons.org/licenses/by/4.0/).

exerted antitumor activity *in vivo*. Our findings enlighten both the cellular functions including the NF-κB signaling pathway and the cytotoxic mechanism affected by dioncophylline A.

Introduction

Acute myeloid leukemia (AML) is a form of blood cancer characterized by excessive proliferation and abnormal differentiation of myeloid cells (myeloblasts) in the bone marrow and in peripheral blood. This heterogeneous disease is caused by recurrent genetic mutations including chromosomal aberrations (inversions/deletions), internal tandem duplications, or even complex karyotypes. It is the most common form of acute leukemia among adults and its incidence increases progressively with age (De Kouchkovsky and Abdul-Hay, 2016). The prognosis of AML is classified as good, intermediate, or poor based on the patient's cytogenetic profile. Despite advances in molecular biology and high-throughput screening, the backbone of AML treatment is still based on the combination of cytarabine and anthracycline (Tallman et al., 2005). Although many natural products have proven efficacy as chemotherapeutic agents, only few of them are approved for clinical AML treatment (Hwang et al., 2019).

One emerging class of biologically active secondary metabolites are the naphthylisoquinoline (NIQ) alkaloids such as dioncophylline A (Cpd. **1**, for the structure, see supplementary file 1) (Feineis and Bringmann, 2023; Lombe et al., 2019; Tajuddeen and Bringmann, 2021). They are produced by lianas belonging to the paleotropical plant families Ancistrocladaceae and Dioncophyllaceae, which are indigenous to the rain forests of West, Central, and East Africa, and Southeast Asia. These compounds are known for their pronounced anti-infective activities against protozoan pathogens that cause tropical diseases such as malaria, trypanosomiasis, and leishmaniasis (Feineis and Bringmann, 2023; François et al., 1997; Lombe et al., 2017; Moyo et al., 2020; Ponte-Sucre et al., 2007; Tajuddeen and Bringmann, 2021; Tajuddeen and Van Heerden, 2019). Depending on their individual structures, NIQ alkaloids can also display strong cytotoxicity against PANC-1 human pancreatic cancer cell lines, INA-6 multiple myeloma cells, or against drug-sensitive (CCRF-CEM) and multidrug-resistant leukemia cell lines (CEM/ADR5000) (Awale et al., 2018; Fayez et al., 2021, 2019, 2018; Li et al., 2017a, 2017b; Tshitenge et al., 2018).

The transcription factor nuclear factor κ B (NF-κB) plays an essential role in multiple cellular processes by regulating the expression of genes involved in cell growth, metastasis, angiogenesis, and suppression of apoptosis (Lin and Karin, 2003). Hence, several studies performed *in vitro* and *in vivo* introduced the NF-κB inhibition strategy as an important approach for the treatment of hematological malignancies and other types of cancers. This strategy can be applied alone or in combination with another chemotherapy (Baud and Karin, 2009). Under physiological conditions, NF-κB is bound to IκB to block its function. Activation of the IκB kinase (IKK) complex by specific stimuli leads to phosphorylation of IκBα (Xia et al., 2014). Then, the ubiquitination process and the proteasome-mediated degradation of IκBα take place, leaving NF-κB free to translocate to the nucleus and to bind to the promoter region of NF-κB-related genes and to upregulate their expression (Dawood et al., 2019a).

There is a lack of understanding in the molecular mechanism of the NIQ alkaloids although they are known to have strong cytotoxic activity in various cancer cells. So far, there is no study evaluating in depth the activity of dioncophylline A on leukemia cells and its mechanism of action. Aiming to shed light on this, in the current study we focused on the NF-κB signaling pathway as it is involved broadly in cancer development and progression as mentioned above (Xia et al., 2018a).

In this paper, we report on the anti-leukemic activity of selected 7,1′-coupled natural and unnatural naphthylisoquinolines related to the plant alkaloid dioncophylline A (Cpd. **1**) as the parent compound (Bringmann et al., 1990a, 1990b). Among the substances tested against CCRF-CEM and CEM/ADR5000 cells were its two likewise naturally occurring regioisomeric monophenolic analoques, 4′-*O*-demethyldioncophylline A (Cpd. **2**) and 5′-*O*-demethyldioncophylline A (Cpd. **3**) (Bringmann et al., 2013). In addition, an unnatural analogue of Cpd. **1**, 8-*O*-(*p*-nitrobenzyl)dioncophylline A (Cpd. **4**) (supplementary file 1) (Bringmann et al., 1997) was studied. Here, we describe for the first time the mechanism of action of the activity of dioncophylline A using microarray and Ingenuity Pathway Analysis (IPA)™. Bioinformatic analysis showed NF-κB as top network of the genes deregulated by Cpd. **1.** We further explored the inhibition of NF-κB pathway *in silico* and *in vitro*. Additionally, Cpd. **1** blocked the translocation of NF-κB to the nucleus. Likewise evaluated was the effect of Cpd. **1** towards NF-κB-related cellular processes. Furthermore, the antitumor activity of Cpd. **1** was tested *in vivo*, using a xenograft zebrafish model.

Materials and methods

Preparation of the naphthylisoquinolines

Dioncophylline A (Cpd. **1**) was obtained by isolation from the West African liana Triphyophyllum peltatum (Bringmann et al., 1990a). Plant material of Triphyophyllum peltatum (Hutch. & Dalz.) was collected in the Parc de Tai (West Ivory Coast) and identified by Prof. l. Aké Assi, Centre National der Floristique, Abidjan; a voucher specimen has been deposited at Herbarium Bringmann, University of Würzburg (No. 02). By stereoselective total synthesis (Bringmann et al., 1990b), while the O-demethylated alkaloids (Cpds. **2** and **3**), which also occur in nature, were prepared by semi-synthesis from Cpd. **1**, by *O*-demethylation and chromatographic resolution of the two resulting regioisomers by HPLC on a Symmetry RP-18 phase (Bringmann et al., 2013). The unnatural analogue Cpd. **4** was prepared from Cpd. **1** by selective 8-*O*-alkylation following a procedure described earlier (Bringmann et al., 1997).

Cytotoxicity assay

The cytotoxicity of dioncophylline A (Cpd. **1**) and its three naphthylisoquinoline derivatives, Cpds. **2**–**4**, was measured using the resazurin (Promega, Mannheim, Germany) reduction assay (Kuete and Efferth, 2013) using DMSO as negative control. The principle of this assay is that living cells can metabolically reduce the non-fluorescent dye resazurin to give the fluorescent dye resorufin (O'Brien et al., 2000). CCRF-CEM cells and CEM-ADR5000 cells were kindly provided by Prof. Axel Sauerbrey (Department of Pediatrics, University of Jena, Germany), HEK-Blue™ Null1 cells (Invivogen, San Diego, CA, USA), and human peripheral blood mononuclear (PBMC) cells which were isolated as described by previously (Saeed et al., 2018). All cells were seeded (1×10^5 cells/well) into 96-well culture plates, then treated with different concentrations of the respective naphthylisoquinoline and incubated for 72 h at 37 °C, except for HEK-Blue™ Null1 cells, which had to be seeded 24 h prior to the treatment step for the attachment. Then, 20 µl of 0.01% w/v resazurin (Sigma-Aldrich, Schnelldorf, Germany) were added to each well and incubated again for 4 h at 37 °C. The resazurin fluorescence was detected at an excitation wavelength 544 nm and an emission at 590 nm using an Infinite M2000 Pro-plate reader (Tecan, Crailsheim, Germany). The percentage of cell viability was calculated as follows:

Cell viability (% of control) = (absorption (treated cells) − absorption (medium alone) / absorption (untreated cells) − absorption (medium alone)) × 100

IC_{50} values were calculated in comparison to the DMSO-treated control and from the concentration dependent curves using nonlinear regression analysis tool built in Excel 2020 software. This assay was

repeated three times with six wells for each concentration. IC_{50} values were expressed as the mean ± standard deviation (SD).

RNA isolation and microarray hybridization

The leukemia cell line CCRF-CEM was treated for 24 h with dioncophylline A (Cpd. **1**) at its IC_{50} concentration. Then, total RNA of treated and untreated cells was extracted using the RNeasy Kit from Qiagen (Hilden, Germany) according to the manufacturer's instructions. The reverse transcription reaction was performed to convert the isolated RNA to cDNA. For this purpose, 1.0 µg RNA template was converted into cDNA with the Luna Script™ RT SuperMix Kit (E3010) purchased from New England Biolabs GmbH, following the manufacturer's protocol. Microarray hybridizations were carried out for treated samples and control samples as previously described in detail (Abdelfatah et al., 2022). The quality of the samples was controlled by the Genomics and Proteomics Core Facility at the German Cancer Research Center (DKFZ, Heidelberg, Germany) prior to the microarray hybridizations on Illumina Human HT-12 BeadChip arrays (Illumina, San Diego, CA, USA).

Ingenuity pathway analysis (IPA)™

The deregulated genes based on microarray hybridizations were uploaded into the Chipster™ program (https://chipster.csc.fi) for further data processing (Mahmoud et al., 2018). The filtered data were imported to IPA to identify biological pathways, functions relevant to the deregulated genes, upstream regulators, and networks. A core analysis was constructed with default parameters except for the statistical cut-off, which was set to a value of $p < 0.05$. Networks were created and the upstream regulator was analyzed based on the deregulated genes. The global canonical pathways involved in cells treated with dioncophylline A (Cpd. **1**) were generated according to the Ingenuity Pathway Knowledge Data Base.

Molecular docking

The 3D structure of dioncophylline A (Cpd. **1**) was downloaded from the PubChem database (https://pubchem.ncbi.nlm.nih.gov/compound/Dioncophylline-A) in the spatial data file (SDF) format. 3D structures of the derivatives of dioncophylline A, Cpds. **2**–**4**, were created by making manual modifications on the SDF file of dioncophylline A (Cpd. **1**), followed by an energy minimization step using ChemDraw3D (https://perkinelmerinformatics.com/products/research/chemdraw) and saved as a Protein Data Bank (PDB) file. All 3D structures of Cpds. **1–4** thus generated were confirmed by one of the authors (G.B.). Triptolide was utilized as a positive control. To generate its structure, the same procedure was applied as above (Bockers et al., 2020).

NF-κB p65/p50 heterodimer:IκBα complex (PDB: 1NFI) was downloaded from the Protein Data Bank (https://www.rcsb.org/) as a PDB file. The inhibitor IκBα chain and the p50 chain were deleted, water molecules and heteroatoms were removed, polar hydrogens and Kollman charges were added and then converted to a pdbqt file using AutoDockTools 1.5.6 (https://ccsb.scripps.edu/mgltools/). The grid box was as follows (spacing: 0.4; x, y, z centers: 3.348, 44.715, 17.684, and the x, y, z dimensions: 80, 70, 126). All required maps, gpf, glg and dpf files were generated by AutoDockTools. The Lamarckian algorithm was exerted with 250 runs and 2500,000 energy evaluations. Molecular docking was carried out using the supercomputer Mogon and advisory services offered by the Johannes Gutenberg University, Mainz (hpc.uni-mainz.de), which is a member of the AHRP (Alliance for High-Performance Computing in Rhineland-Palatinate, ahrp.info) (Kadioglu et al., 2021).

Table 1
Primers sequences of selected genes for qRT-PCR.

Gene	Forward primer	Reverse primer
ETV5	5′AGCTGTCTCTGGATTGGCAC3′	5′TTTGGTGGTTTTCTGCCCCT3′
DDIT4L	5′TCCTGAACCCAACCTCAACG3′	5′AAAGCCGCAGGACATCTTGA3′
IGLL3P	5′GGCAGATTTCAGAGGCCCTT3′	5′CAGTAGGTCCCAGCAACTCC3′
ID1	5′GTGCCTAAGGAGCCTGGAAA3′	5′CCGCCTGTGAAAACGAGAAG3′
SLC32A1	5′CGGCAGCTCCGCAGT3′	5′GCGTTCGAGGCTCTCTCAG3′
LST1	5′TGGCCCAGGGCTCCTC3′	5′GCAATGCAGGCATAGTCAGC3′

Quantitative real-time reverse transcription PCR

The qPCR method was applied to validate the microarray result. Ready master mix (5 × Hot Start Taq EvaGreen® qPCR Mix (no ROX)) was purchased from Axon Labortechnik, Kaiserslautern, Germany, for the gene amplification procedure. The PCR primers for the top deregulated genes were designed and verified using NCBI/Primer-BLAST and then purchased from Eurofins MWG Operon (Ebersberg, Germany). Primer sequences and their annealing temperatures are listed in Table 1. The housekeeping gene glyceraldehyde-3-phosphate dehydrogenase (*GAPDH*) was used as an endogenous control.

Using CFX384™ (Bio-Rad, Munich, Germany), 40 cycles were carried out in 384-well plates. The amplification cycles were set with the following conditions: denaturation step at 95 °C for 15 s, gradient annealing temperatures at 62–47 °C for 30 s, and elongation temperatures at 72 °C for 1 min. The Cq values were determined using CFX Manager Software (version 3.1; Bio-Rad) (Gillet et al., 2004). The final fold change was calculated using the 2-ΔΔCt method after normalizing gene expression to the expression of control GAPDH of the respective samples (Livak and Schmittgen, 2001).

NF-κB reporter assay

The NF-κB SEAP reporter parental cell line HEK-Blue™ Null1 was purchased from InvivoGen (San Diego, CA, USA) and cultured under the recommended conditions. The cells were originally transfected with secreted embryonic alkaline phosphatase (*SEAP*) reporter gene, its expression was controlled by the NF-κB promoter sequence. A total of 1×10^5 NF-κB SEAP reporter HEK-Blue™ Null1 cells were seeded in 96-well plates and incubated for 24 h, allowing the attachment. The HEK-Blue™ Null1 cells were treated with three different concentrations of the four naphthylisoquinolines, Cpds. **1–4**, for 24 h. Then, 100 ng/ml of tumor necrosis factor (TNF) were added to the cells for 24 h to activate NF-κB. An Infinite M2000 Pro-Plate Reader was used at 630 nm to quantify SEAP levels using pre-warmed Quanti-Blue reagent from InvivoGen. As a positive control, triptolide (1 M, InvivoGen) was used (Dawood et al., 2019b). The assay was performed three times.

Annexin-V/PI double staining

CCRF-CEM cell lines in growth phase were seeded (1×10^6 cells/well) in 6-well plates provided with 2 ml RPMI medium. The cells were treated with three different concentrations of dioncophylline A (Cpd. **1**). After 48 h, annexin V-FITC/PI double staining kit (Invitrogen, Life Technologies GmbH, Darmstadt, Germany) was used to detect the induction of apoptosis as previously described (Hegazy et al., 2020). Cells treated with dioncophylline A or DMSO were centrifuged and resuspended in PBS. The cells were centrifuged again, and the cell pellet was washed using 1 × binding buffer provided by the kit. Then, annexin V-FITC was added to the cells for 15 min at room temperature followed by addition of PI staining. Apoptosis was measured using a flow cytometer (BD Accuri™ C6, BD Biosciences, Becton Drive, Franklin Lakes,

US); the FL1 and FL2 detectors were set for FITC and PI, respectively. The annexin-V/PI double staining experiments were performed three times.

Detection of autophagy

Autophagy was performed using the Autophagy Detection Kit (ab139484, Abcam) according to the manufacturer's protocols. CCRF-CEM cells were treated with different concentrations of dioncophylline A (Cpd. **1**) and rapamycin for 24 h. Assay buffer, as included in the Autophagy Detection Kit, was used to wash the cells twice. After centrifugation, the cell pellets were re-suspended in 250 µl of indicator-free cell culture media supplemented with 5 % FBS, and the cells were incubated at 37 °C for 30 min in another 250 µl of medium containing green stain solution (included in the Autophagy Detection Kit). The cells were washed again with the assay buffer and re-suspended in 500 µl assay buffer. A standard green (FL1) filter was set in the BD Accuri™ C6 flow cytometer to detect the autophagic signal (Abdelfatah et al., 2019).

Cell cycle analysis using propidium iodide (PI)

A total of 1×10^6 CCRF-CEM cells were seeded in 6-well plates followed by the treatment step with three different concentrations of dioncophylline A (Cpd. **1**) for 24 h. DMSO-treated cells served as the negative control. Cells were harvested using centrifugation at 350 × g for 5 min at 10 °C and washed with cold PBS. The cell pellet was then fixed with ice-cold aqueous 75 % ethanol and stored at –20 °C for at least 3 h. The fixed cells were then washed with PBS and treated with 5 µg RNAse (Merck KGaA, Germany). Finally, the cells were stained with propidium iodide (PI, 50 µg/ml) (Merck KGaA, Germany) diluted in PBS. The cell cycle phases were analyzed using a BD Accuri™ C6 Flow Cytometer (BD Biosciences) (Abdelfatah et al., 2019). Every experiment was carried out at least twice.

Endothelial tube formation assay

The activity of dioncophylline A (Cpd. **1**) on angiogenesis was measured using the tube-formation assay. µ-Slide angiogenesis (ibidi GmbH, Martinsried, Germany) was covered with 10 µl of Matrigel® (Corning GmbH, Kaiserslautern, Germany) and incubated for polymerization for 30 min. Then, 1×10^4 cells/well of human umbilical vein endothelial cells (HUVECs) which were kindly provided by Dr. Ronald E. Unger (Repair-Lab, Institute of Pathology, University Medical Center of Johannes Gutenberg University Mainz, Mainz, Germany) added with 30 ng/ml VEGF (Promocell, Heidelberg, Germany) were seeded on polymerized Matrigel®. The cells underwent the treatment of dioncophylline A (Cpd. **1**) with the concentration of 1, 5, and 10 µM, respectively, or DMSO as the solvent control for 16–18 h at 37 °C in a humidified chamber with 5 % CO_2 to allow tube formation. The wells were washed three times with Hank's balanced salt solution (HBSS) (Corning B. V. Life Sciences) after staining with 6.25 µg/ml Calcein-AM (Cayman Chemical, USA) for 30 min at room temperature. Fluorescent images were taken at 485 nm / 529 nm by an AF7000 widefield fluorescence microscope at the Microscopy & Histology Core Facility at IMB (Mainz, Germany). The Image Analysis Platform of Wimasis (https://mywim.wimasis.com/) was utilized for analyzing the tube length and branching points (Mahmoud et al., 2022).

Immunofluorescence assay and confocal laser scanning microscopy analysis

HEK-Blue™ Null1 cells were seeded in chamber slides (Nunc) and treated with different concentrations of dioncophylline A (Cpd. **1**) and triptolide for 24 h. The cells were washed three times with cold PBS followed by a fixation step with 4 % paraformaldehyde solution in PBS for 20 min. The fixed monolayer cells were washed three times with PBS and incubated with 0.25 % Triton X-100 for 10 min followed by a blocking step using 3 % bovine serum albumin for 1 h. Then, anti-NF-κB antibody (1:200, D2E5, Cell Signaling, Frankfurt am Main, Germany) was diluted in blocking buffer and added to the washed cells and incubated for 24 h at 4 °C. The slides were then washed three times, 5 min each, with PBS followed by addition of secondary antibody Alexa Fluor 488-conjugated anti-rabbit (1:700, Invitrogen, A11032, Darmstadt, Germany). Additionally, the cells were stained with 2 µg/ml 4′,6-diamidino-2-phenylindole (DAPI) (Sigma-Aldrich) and mounted in Fluoromount-G® (SouthernBiotech, Birmingham, AL, USA) (Dawood et al., 2020a; Trask, 2004). The stained slides were imaged by AF7000 Widefield Fluorescence Microscope (40 × magnification).

Zebrafish preparation

The Institute of Hydrobiology, Chinese Academy of Science (Wuhan, China), kindly provided the wild-type AB zebrafish strain, which has been approved by the Association for Assessment and Accreditation of Laboratory Animal Care (AAALAC) International (SYXK 2012–0171). By natural pair-mating, zebrafish larvae were obtained 48 h post fertilization (hpf). The larvae were maintained in a light-controlled aquaculture facility with a typical 14:10 h day/night photoperiod. They were fed live brine shrimp twice daily and dry flakes once daily. The culture condition was as following, 0.2 % immediate ocean salt, pH 6.5–8.5, conductivity 450–550 S/cm, and hardness 50–100 mg/l $CaCO_3$, the temperature of the water was kept constant at 28 °C (Dawood et al., 2020b).

Determination of the No Observed Adverse Effect Level (NOAEL) of dioncophylline A

To determine the dose range of dioncophylline A (Cpd. **1**), a total of 240 zebrafish larvae at 72 h post-fertilization (hpf) were used, divided into eight groups, with 30 fish in each group, in 6-well plates (Nest Biotech, China). Dioncophylline A was dissolved in DMSO for the treatment groups, and DMSO alone was used for the normal control group. Zebrafish groups were microinjected with different concentrations of dioncophylline A (0.156, 0.312, 0.625, 1.25, 2.50, and 5.00 µM) for 48 h and incubated at 35 °C. All fish were visually observed, and images were taken under a dissecting stereomicroscope (Olympus Ltd., Tokyo, Japan). Dead zebrafish were counted and removed every day, and adverse events of zebrafish were recorded for each group (Dawood et al., 2020b). Finally, the NOAEL was estimated for the xenograft anti-cancer experiment.

Statistical analysis

The statistical tests were carried out using GraphPad Prism version 8.0. Statistical significance evaluation was done by *t*-test comparing two groups in an experiment. P-values less than 0.05 were deemed significant and displayed as one asterisk (*) while the p-values less than 0.01 were presented as two asterisk (**) and the p values less than 0.001 were considered statistically highly significant and exhibited as three asterisks (***). Error bars, unless otherwise noted, display the standard error of three separate studies.

Results

Naphthylisoquinoline derivatives inhibit cancer cell growth

The cytotoxicity profiles of dioncophylline A (Cpd. **1**) and its derivatives, Cpds. **2–4**, were assessed on CCRF-CEM and multidrug-resistant CEM/ADR5000 cell lines using the resazurin assay. Dioncophylline A (Cpd. **1**) as the parent alkaloid and the by far most active among the tested compounds exhibited the lowest IC_{50} values, 0.46 ± 0.01 µM and 0.69 ± 0.04 µM for the two used cell lines, respectively. 8-*O*-(*p*-Nitrobenzyl)dioncophylline A (Cpd. **4**) was the second active

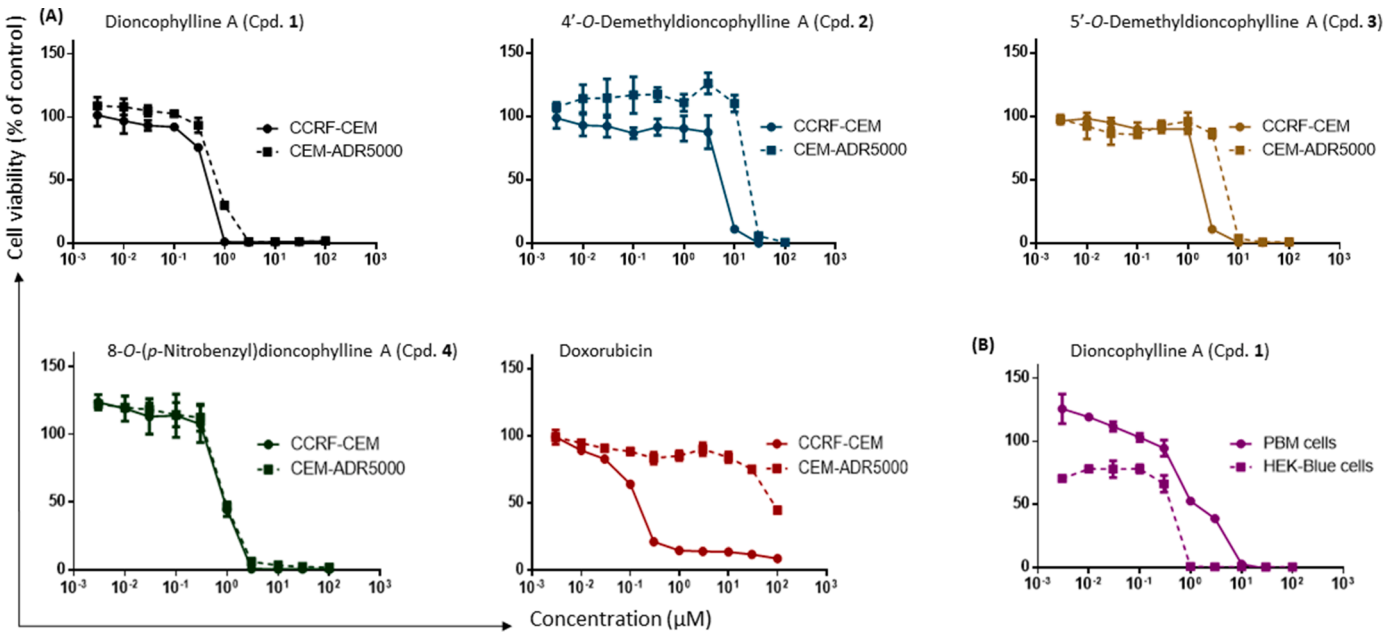

Fig. 1. Cytotoxic effect of naphthylisoquinolines, Cpds. **1**–**4**, by the resazurin assay. (A) Dose-response curves of dioncophylline A and its derivatives, with the positive control doxorubicin on CCRF-CEM and CEM-ADR5000 cells. (B) Cytoxicity of dioncophylline A on normal healthy cells (PBMC) and HEK-Blue™ Null1 cells upon dioncophylline A treatment. The data are the result of mean values ± SD of three independent experiments.

compound, while the 4′- and 5′-*O*-demethyl derivatives (Cpds. **2** and **3**, respectively) had higher IC_{50} values with less activity, as illustrated in Fig. 1A. Taking the degree of resistance into consideration, 8-*O*-(*p*-nitrobenzyl)dioncophylline A (Cpd. **4**) and dioncophylline A (Cpd. **1**) exerted values of 1- and 1.5-fold while the positive control doxorubicin was 580-fold. The results with the IC_{50} values for two cell lines and the degree of resistance are presented in Table 2.

As shown in Fig. 1B, dioncophylline A inhibited the human peripheral mononuclear cells (PBMC) with an IC_{50} value of 1.2 ± 0.03 μM, while HEK-Blue™ Null1 cells displayed a lower IC_{50} value of 0.40 ± 0.04 μM. PBMC was less sensitive to dioncophylline A (Cpd. **1**) compared to the two leukemic cell lines (CCRF-CEM and CEM/ADR5000).

Microarray analysis

The microarray-based expression profiling utilizing the Chipster software revealed a deregulation of a total of 282 genes in CCRF-CEM cells. IPA network analysis predicted NF-κB as the top network of the deregulated genes by dioncophylline A (Fig. 2). Null activity was observed on the cells with the negative control DMSO. Nearly all genes that are connected to NF-κB complex were downregulated, while other genes, such as the one connected to interferon-α, were upregulated. Interestingly MAPK1, which is upregulated in many cancer types, was also downregulated in this case (Li et al., 2017c). Further analyses by IPA were performed to identify cellular functions and canonical pathways that are affected by the treatment with dioncophylline A (Cpd. **1**), and showed that cell cycle progression and angiogenesis were particularly inhibited.

Correlation between qRT-PCR and microarray results

Confirmation of the microarray method was performed using qRT-PCR analysis. The activity of dioncophylline A (Cpd. **1**) on the expression of the genes was measured in CCRF-CEM cells by qRT-PCR. As demonstrated in Fig. 3A, treatment of CCRF-CEM by dioncophylline A resulted in significant upregulation of *DDIT4L* and *ETV5* corresponding with the results of microarray analyses. In addition, down-regulation of mRNA expression of *LST1, ID1* and *SLC32A1* genes was observed upon dioncophylline A treatment. The fold change values from both the microarray hybridization and qRT-PCR were subjected to the Pearson correlation test (Fig. 3B). The outcome confirmed a significant correlation between the two methods with an R-value of 0.98, providing the validation of the microarray technique.

In silico binding of dioncophylline A to NF-κB and inhibition of its activity in vitro

Molecular docking, a crucial tool in the area of computer-aided drug design, was performed to see possible interaction sites of dioncophylline A (Cpd. **1**) and its derivatives to NF-κB. The lowest binding energies, predicted inhibition constants, and the interacting amino acids are listed in Table 3. The binding energies were shown to be about −7 kcal/mol for three of the compounds, **1–3**, while 8-*O*-(*p*-nitrobenzyl)

Table 2
Cytotoxic effects of naphthylisoquinoline alkaloids towards leukemia cell lines.

Compounds names	IC_{50} in CCRF-CEM (μM)	CEM/ADR5000 (μM)
Dioncophylline A (Cpd. **1**)	0.46 ± 0.01	0.69 ± 0.04
4′-*O*-Demethyldioncophylline A (Cpd. **2**)	5.37 ± 0.59	18.41 ± 0.65
5′-*O*-Demethyldioncophylline A (Cpd. **3**)	1.75 ± 0.05	5.10 ± 0.14
8-*O*-(*p*-Nitrobenzyl)dioncophylline A (Cpd. **4**)	0.90 ± 0.10	0.94 ± 0.06
Doxorubicin	0.14 ± 0.004	81.24 ± 6.32

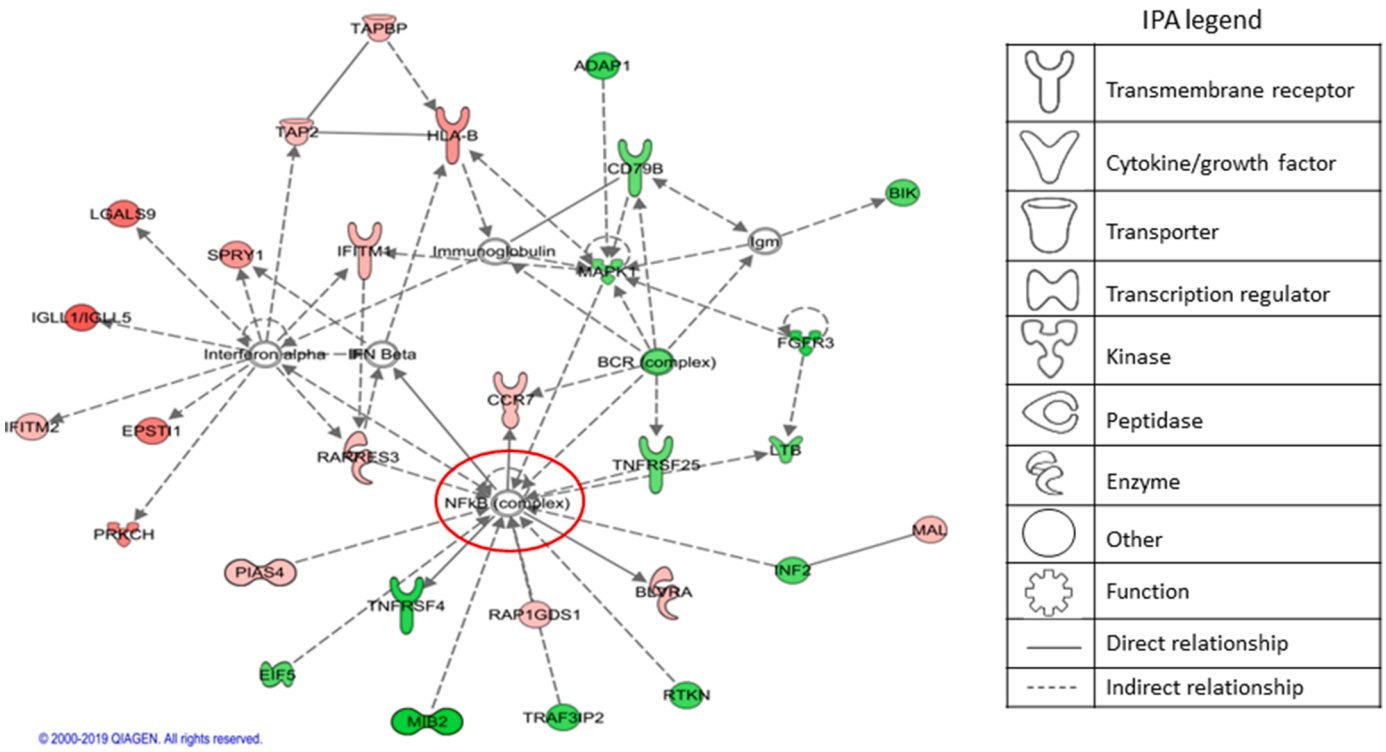

Fig. 2. Microarray analysis using IPA. Deregulated genes in dioncophylline A treated CCRF-CEM cells hint at the NF-κB pathway. The color green indicates downregulation, while the color red represents upregulation.

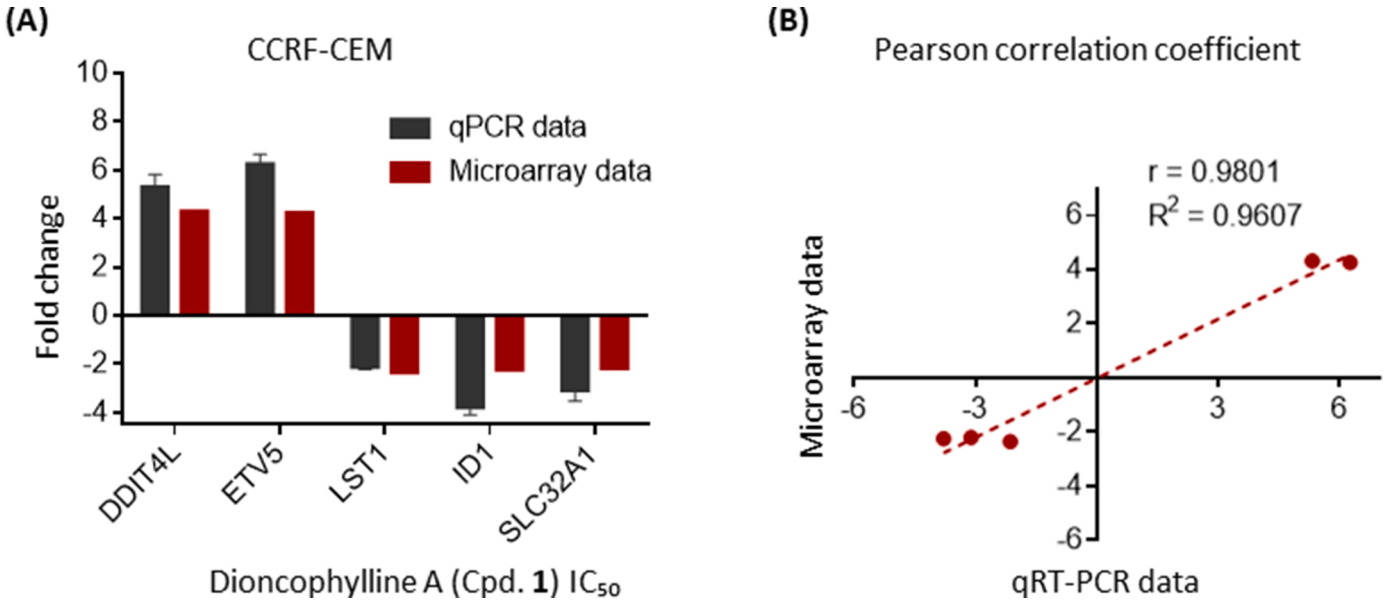

Fig. 3. Validation of microarray-based gene expression by RT-qPCR. (A) Fold change, which represents expression levels of five selected genes upon the treatment of dioncophylline A. (B) Pearson r-value > 0.90 indicates that the results of RT-qPCR highly correlate with the microarray assay. Each analysis was executed three times independently in duplicate.

Table 3
Binding energies and predicted inhibition constants (pKi) are represented as mean ± SD as well as amino acids that are involved in the interaction of the ligand.

Compound	Mean binding energy (kcal/mol)	pKi (μM)	Pharmacophore
8-*O*-(*p*-nitrobenzyl)dioncophylline A	−10.18 ± 0.11	0.034 ± 0.006	LYS26, LYS28, MET32, ARG35, ALA43, GLY44, SER45, PRO47, HIS58
4′-*O*-Demethyldioncophylline	−7.65 ± 0.24	2.600 ± 0.922	ARG35, ARG41, SER42, ALA43, GLY44, VAL91, GLN119
Dioncophylline A	−7.55 ± 0.10	2.947 ± 0.502	ARG35, ARG41, ALA43, GLY44, VAL91, GLN119
5′-*O*-Demethyldioncophylline	−7.46 ± 0.02	3.397 ± 0.136	ARG35, ARG41, ALA43, GLY44, VAL91, GLN119
Triptolide	−6.15 ± 0.00	31.130 ± 0.070	GLY32, ARG35, ARG41, SER42, ALA43, VAL91,

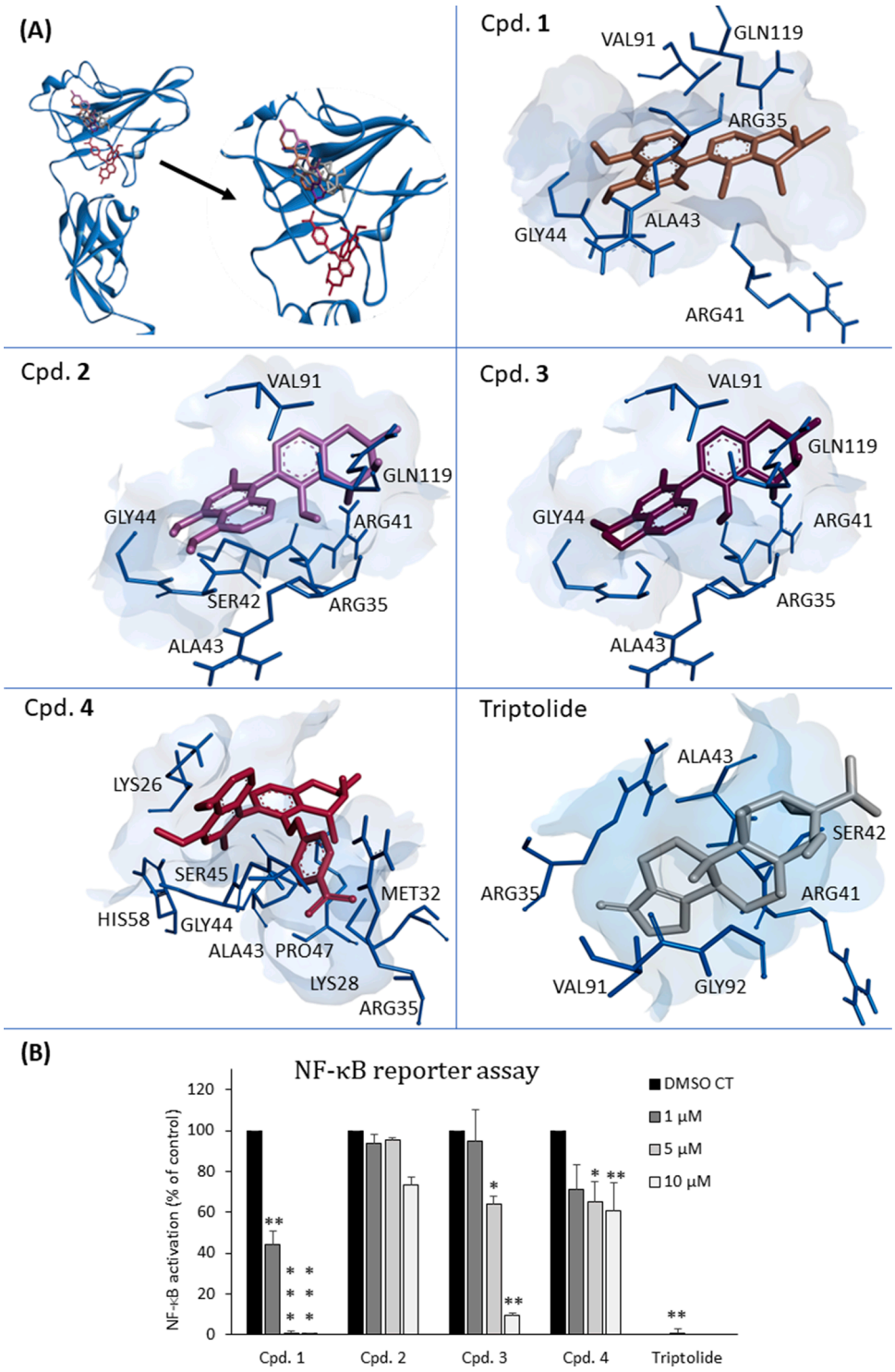

Fig. 4. Molecular docking and *in vitro* NF-κB reporter assay. (A) The docking poses and interacting amino acid residues of NF-κB (PDB ID: 1NFI) with Cpd. **1** (dioncophylline A), Cpd. **2** (4′-*O*-demethyldioncophylline A), Cpd. **3** (5′-*O*-demethyldioncophylline A), Cpd. **4** (8-*O*-(*p*-nitrobenzyl)dioncophylline A), and the positive control triptolide. Each docking was carried out three times. (B) NF-κB activity upon treatment with the respective NIQ derivatives in three concentrations (1, 5, and 10 μM), in comparison with the known inhibitor triptolide. *: $p < 0.05$, **: $p < 0.01$, ***: $p < 0.001$.

dioncophylline A gave a value of −10 kcal/mol. Molecular interactions of the four compounds plus triptolide with the NF-κB are exhibited in Fig. 4. Dioncophylline A (Cpd. **1**) was shown to share the same binding site with the positive control triptolide and also with 4′-*O*-demethyldioncophylline (Cpd. **2**) and 5′-*O*-demethyldioncophylline (Cpd. **3**). As indicated in Fig. 4A, dioncophylline A overlapped with its 4′-*O*- and 5′-*O*-demethyl derivatives in the triptolide binding site, while 8-*O*-(*p*-nitrobenzyl)dioncophylline A (Cpd. **4**) stood close to them but in a different position of the protein.

Aiming to confirm the *in silico* binding of the ligands to NF-κB and the microarray result, NF-κB reporter assay was performed. The reporter cell line HEK-Blue™ Null 1 was treated with concentrations of 1, 5, and 10 μM of four compounds with triptolide as positive control and DMSO as negative control. As demonstrated in Fig. 4B, dioncophylline A (Cpd. **1**)

had an outstanding NF-κB inhibition activity compared to its derivatives, at all tested concentrations. Remarkably, at a concentration of 1 μM, dioncophylline A (Cpd. **1**) lowered NF-κB activity by more than 50% and with 5 and 10 μM almost no NF-κB activity was left. 5′-*O*-Demethyldioncophylline A (Cpd. **3**) had an inhibitory activity with the tested 10 μM concentration, while its regioisomer, 4′-*O*-demethyldioncophylline A (Cpd. **2**), and the 8-*O*-(*p*-nitrobenzyl) derivative, Cpd. **4**, exerted only weak activity. Meanwhile negative control DMSO showed non-significant effect on the NF-κB activity.

Dioncophylline A induces autophagy and, to a slight degree, apoptosis

A different cell death mechanism was analyzed using various dioncophylline A concentrations of 0.5 × IC_{50}, IC_{50}, and 2 × IC_{50}. Autophagy analysis was done using the Autophagy Detection Kit and detected by flow cytometry. The results revealed that dioncophylline A (Cpd. **1**) prompted autophagy at IC_{50} and 2 × IC_{50} concentration with the fold change of 3.8 and 7.6, respectively, while the positive control rapamycin was 5.3 (Fig. 5). On the other hand, apoptosis induction was tested using Annexin-V/PI double staining. The outcome of the experiment showed that dioncophylline A slightly induced apoptosis at 2 × IC_{50}. As demonstrated in Fig. 6, treatment of CCRF-CEM with dioncophylline A for 48 h increased the percentage of early apoptosis in a dose-dependent manner from 2.2% in DMSO control to 6.0% at 2 × IC_{50} concentration. Moreover, the apoptosis proportion did not dramatically increase between IC_{50} and 2 × IC_{50}, but necrosis was doubled. While the negative control DMSO showed non-significant effect on the cells.

Dioncophylline A induces G2/M phase cell cycle arrest

CCRF-CEM cells treated with dioncophylline A were acumulated in the G2/M phase of the cell cycle in a concentration-dependent manner. At IC_{50} concentration, the G2/M phase elevated to 16.2% and with 2 × IC_{50} to 21.7%. A significant increase of the S phase to 72.6% with 2 × IC_{50} concentration was also observed. G0/G1 phase cell population were noticed to be similar for both the concentrations of 0.5 × IC_{50} and IC_{50} and then decrease to be 12.5% at 2 × IC_{50} concentration. Overall the data indicate that dioncophylline A induces cell arrest in G2/M phase as in Fig. 7A. That is in agreement with the transcriptome analysis and IPA data, which predicted an effect of dioncophylline A to cell cycle progression, see Fig. 7B.

Suppression of endothelial cell tube formation by dioncophylline A

Endothelial cell tube formation assay was conducted to evaluate the activity of dioncophylline A (Cpd. **1**) on the progress of angiogenesis, a critical player in cancer progression (Martin et al., 2013). Dioncophylline A was administered in concentrations of 1, 5, and 10 μM to HUVECs, which can form capillary-like structures. As presented in Fig. 8, dioncophylline A significantly decreased the total tube length, total branching, and total loops dose-dependently in comparision to the untreated cells. Angiogenesis cellular function was predicted by IPA for the deregulated genes after the treatment with dioncophylline A as shown Fig. 8B. Tube formation was not effected by negative control DMSO.

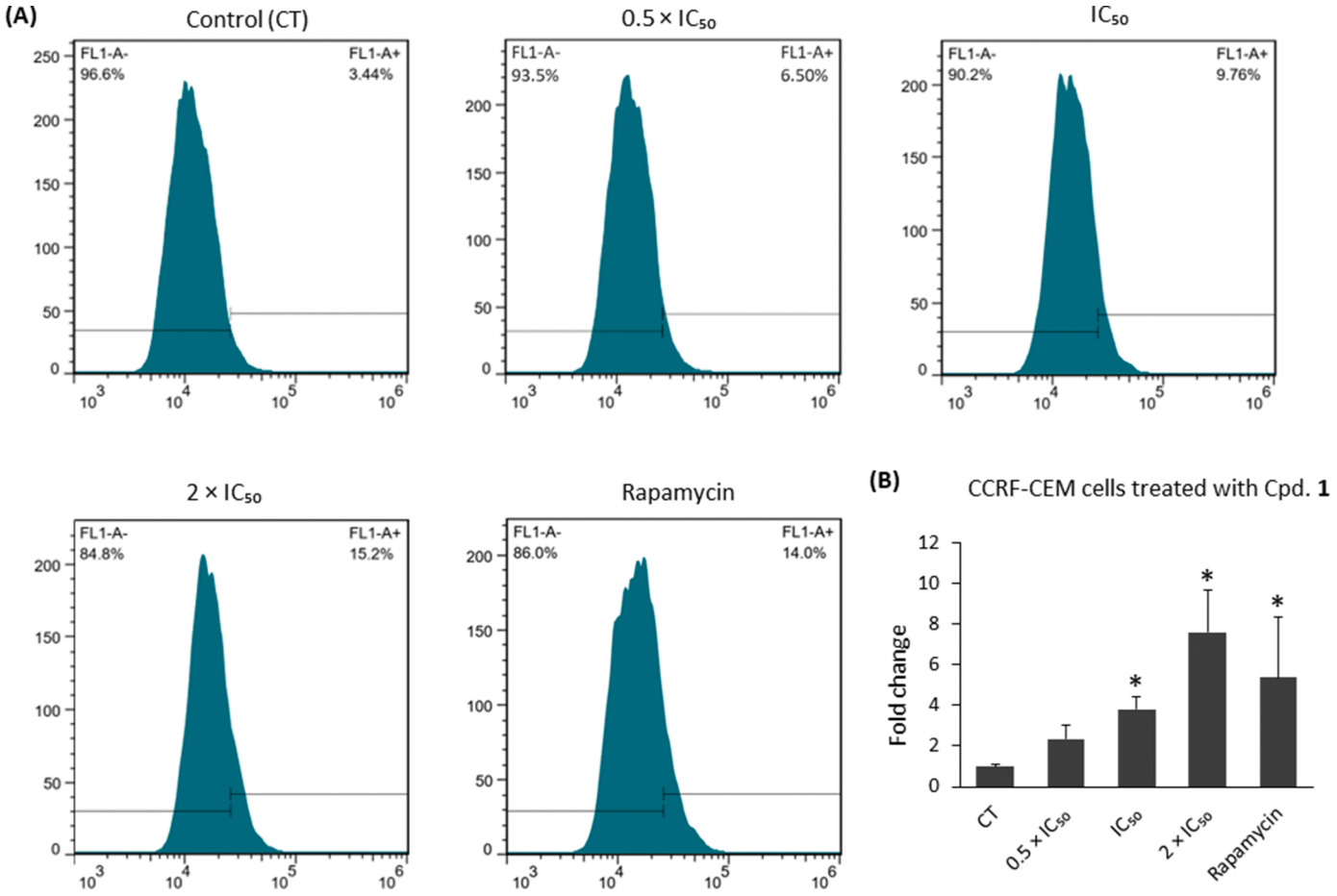

Fig. 5. Autophagy induction by dioncophylline A in CCRF-CEM cells. (A) Flow cytometry histograms showing the alterations induced by the treatment with dioncophylline A (0.5 × IC_{50}, IC_{50}, and 2 × IC_{50}) and the positive control, rapamycin (1 μM) compared to the negative control DMSO. (B) Bar chart illustrating the significant increase in autophagy by dioncophylline A intervention for 24 h in a dose-dependent manner from two independent experiments.

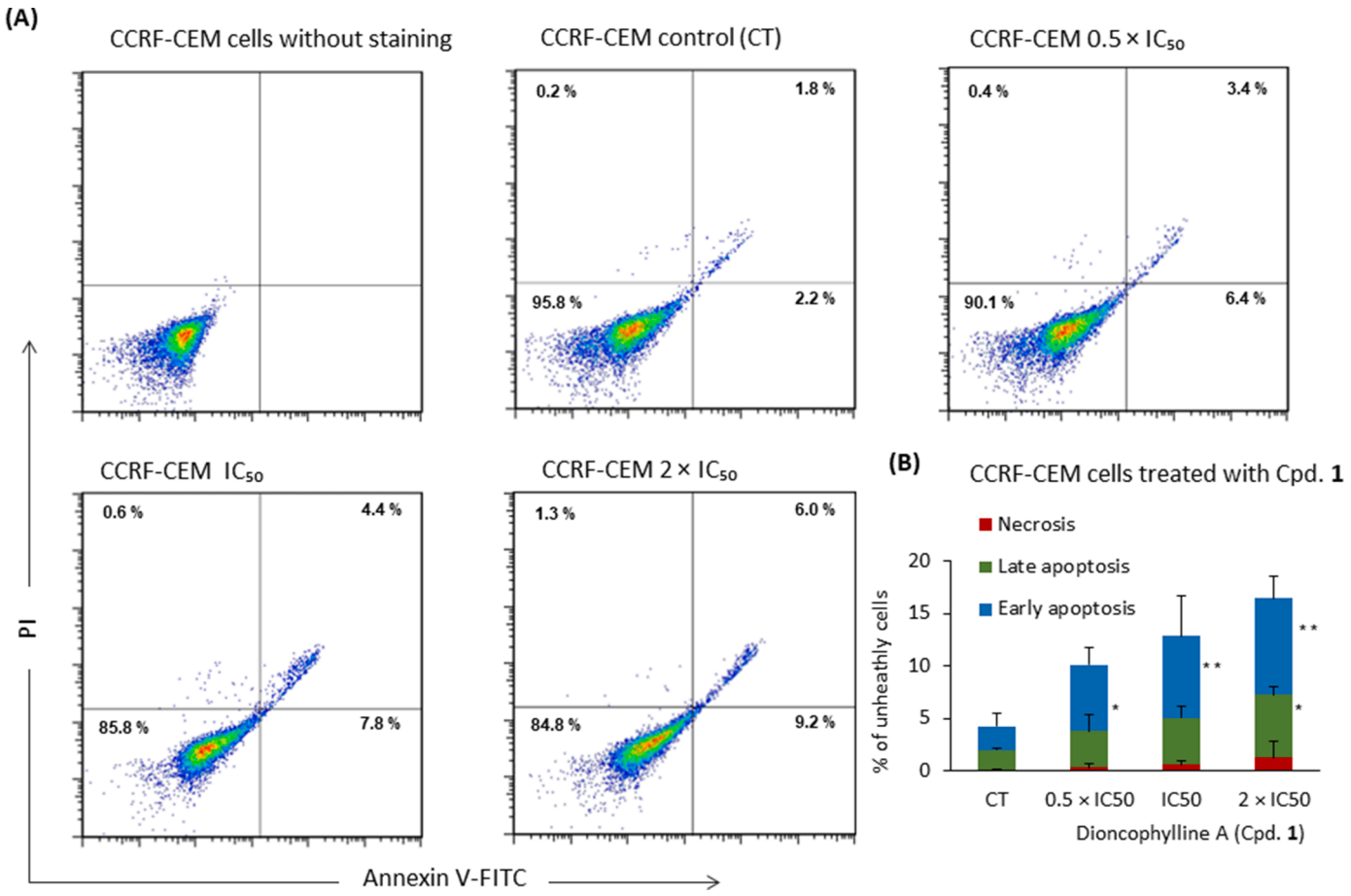

Fig. 6. Analysis of apoptosis by flow cytometry. (A) Slight apoptosis was noticed by annexin V/PI staining in dioncophylline A treated CCRF-CEM cells. The late apoptosis percentage has increased from 2.2 in DMSO control to 9.2 at 2 × IC_{50} concentration while early apoptosis 1.8 to 6.0. (B) The percentage of the cells undergoing necrosis, late and early apoptosis by 48 h treatment with three different concentrations (0.5 × IC_{50}, IC_{50}, and 2 × IC_{50}). The error bars represent mean values ± SD of three independent experiments. *: $p < 0.05$ and **: $p < 0.01$.

Dioncophylline A prevents translocation of NF-κB to the nucleus

The HEK-Blue™ Null1 cells were induced with TNF-α (100 ng/ml) after treatment with 0.5 × IC_{50}, IC_{50}, and 2 × IC_{50} concentrations of dioncophylline A or DMSO for 24 h. Immunofluorescence was used to visualize the NF-κB position inside the cells. Fig. 9 clearly illustrates that in the absence of dioncophylline A, NF-κB translocation from the cytoplasm to nucleus was increased by TNF-α after negative control DMSO was shown to have no effect. However, in cells which were pretreated with dioncophylline A and subsequently treated with TNF-α, the translocation of NF-κB to the nucleus was prevented. These findings supported that dioncophylline A hampers the NF-κB pathway.

In vivo anti-tumor activity of dioncophylline A in a zebrafish model

The zebrafish model was used to screen the anti-cancer activity of dioncophylline A (Cpd. **1**). Six different concentrations of dioncophylline A were tested in zebrafish to evaluate the death rates and adverse events of dioncophylline A in zebrafish larvae. Dioncophylline A (Cpd. **1**) did not show any abnormal phenotypes in a concentration range from 156 to 312 nM (data not shown). Therefore, 312 nM was considered as the NOAEL (No-Observed-Adverse-Effect Level) of dioncophylline A to perform *in vivo* zebrafish experiments. As illustrated in Fig. 10, a CCRF-CEM cell-xenograft model of zebrafish larvae was established, and the cellular fluorescent intensity was applied to calculate the xenograft tumor growth. After 48 h treatment, yolk sac injection of 50.9 nM imatinib mesylate (positive control) as well as two concentrations of dioncophylline A (104 and 312 nM) significantly inhibited CCRF-CEM tumors growth in comparison to the untreated model group which is negative control DMSO.

Discussion

Several studies have demonstrated the cytotoxic effect of NIQ alkaloids (Awale et al., 2018; Fayez et al., 2021, 2019). Recently, Kushwaha et al. found that dioncophylline A has significant anti-tumoral activities on breast cancer cell lines with the IC_{50} value of 1.6 and 0.9 μM for MDA-MB-231 and MCF-7, respectively. Dioncophylline A disrupted mitochondrial membrane potential, increased reactive oxygen species production, and led to apoptosis in two tested cell lines (Kushwaha et al., 2020a). In this study, we investigated, for the first time, the mechanism of action of selected NIQ alkaloids. One of the most potent compounds among a whole series of anti-leukemic NIQ alkaloids tested so far was dioncophylline A (Cpd. **1**) (Li et al., 2017b). It exhibited a strong inhibition of cell proliferation towards CCRF-CEM cells with an IC_{50} value of 0.46 μM, while the standard anti-leukemic drug doxorubicin had a value of 0.14 μM. However, in contrast to the latter, it showed a low degree of cross-resistance against the multidrug-resistant subline CEM/ADR5000 (2.1-fold for Cpds. **1** *versus* 580-fold for doxorubicin), making it a promising drug candidate and warranting further in-depth investigations. In view of the urgent necessity to discover novel anti-cancer agents from natural sources and the fact that dioncophylline A exhibited the best IC_{50} value compared to the other three NIQs, it was investigated more closely using microarray hybridization.

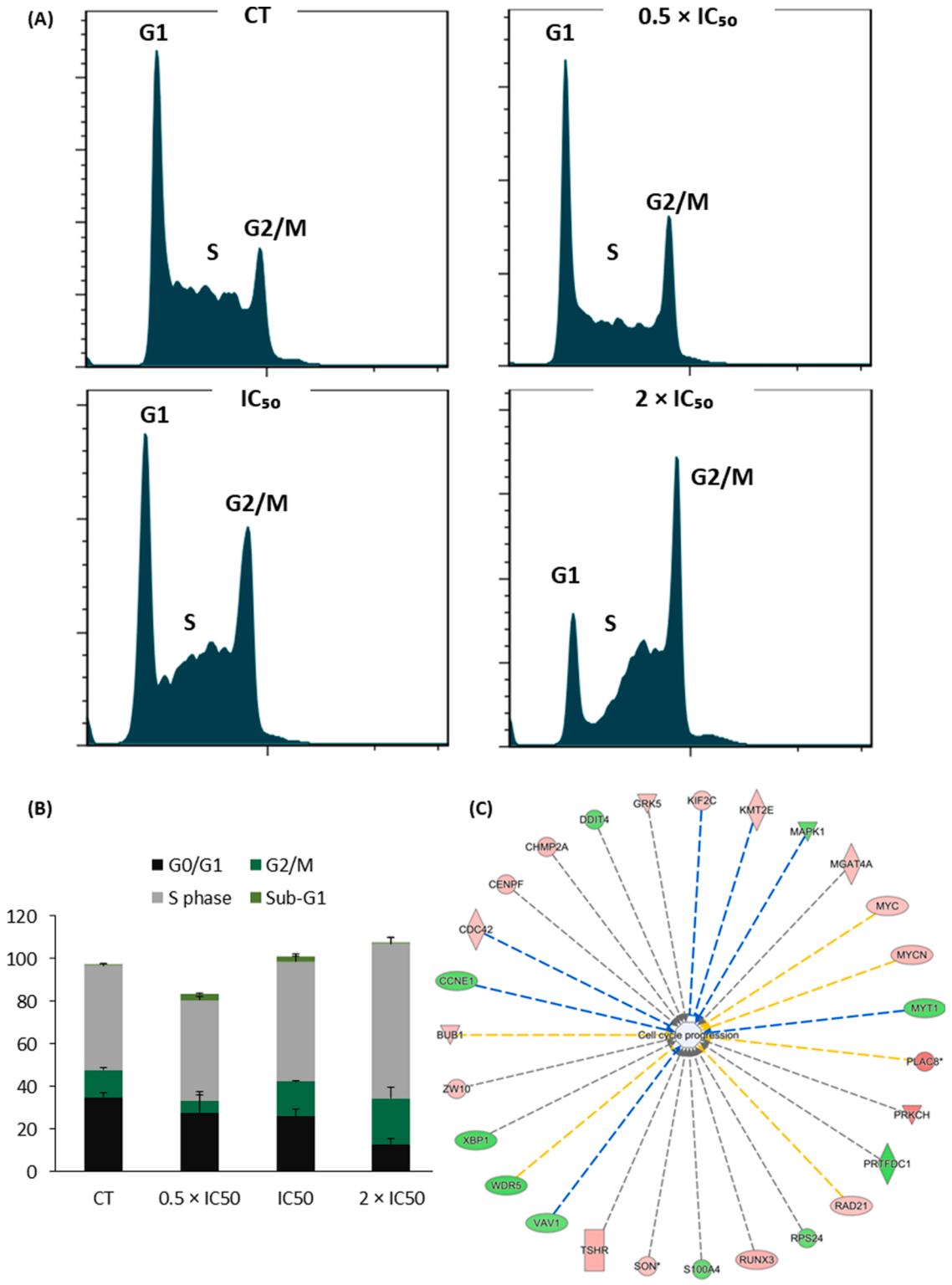

Fig. 7. Cell cycle distribution of CCRF-CEM subjected to dioncophylline A. (A) DNA histograms with three concentrations (0.5 × IC_{50}, IC_{50}, and 2 × IC_{50}) for 24 h. (B) The percentage of cells distributed in different cell cycle phases upon the treatment with dioncophylline A was shown in the bar chart. With a concentration of IC_{50}, the G2/M phase increased to 16.2 %, and at 2 × IC_{50} it reached 21.7 %. Data are shown as mean values ± SD from three independent experiments. (C) Cell cycle-associated molecules identified by IPA upon the treatment with dioncophylline A. Changes in gene expression levels are illustrated using color codes: red indicates upregulation, while green signifies downregulation.

In an attempt to understand the mode of action of dioncophylline A (Cpd. **1**) and its possible cellular functions and the molecular networks that mediate its cytotoxic effect, transcriptomic methods were performed with the RNA gene expression profiles of CCRF-CEM. Previously, whole-transcriptome microarray gene expression analysis had been applied in several studies. Jovanović et al. (2016) studied the response of HeLa cells towards the simple isoquinoline RuT7. They identified several functional categories and signaling and biochemical pathways

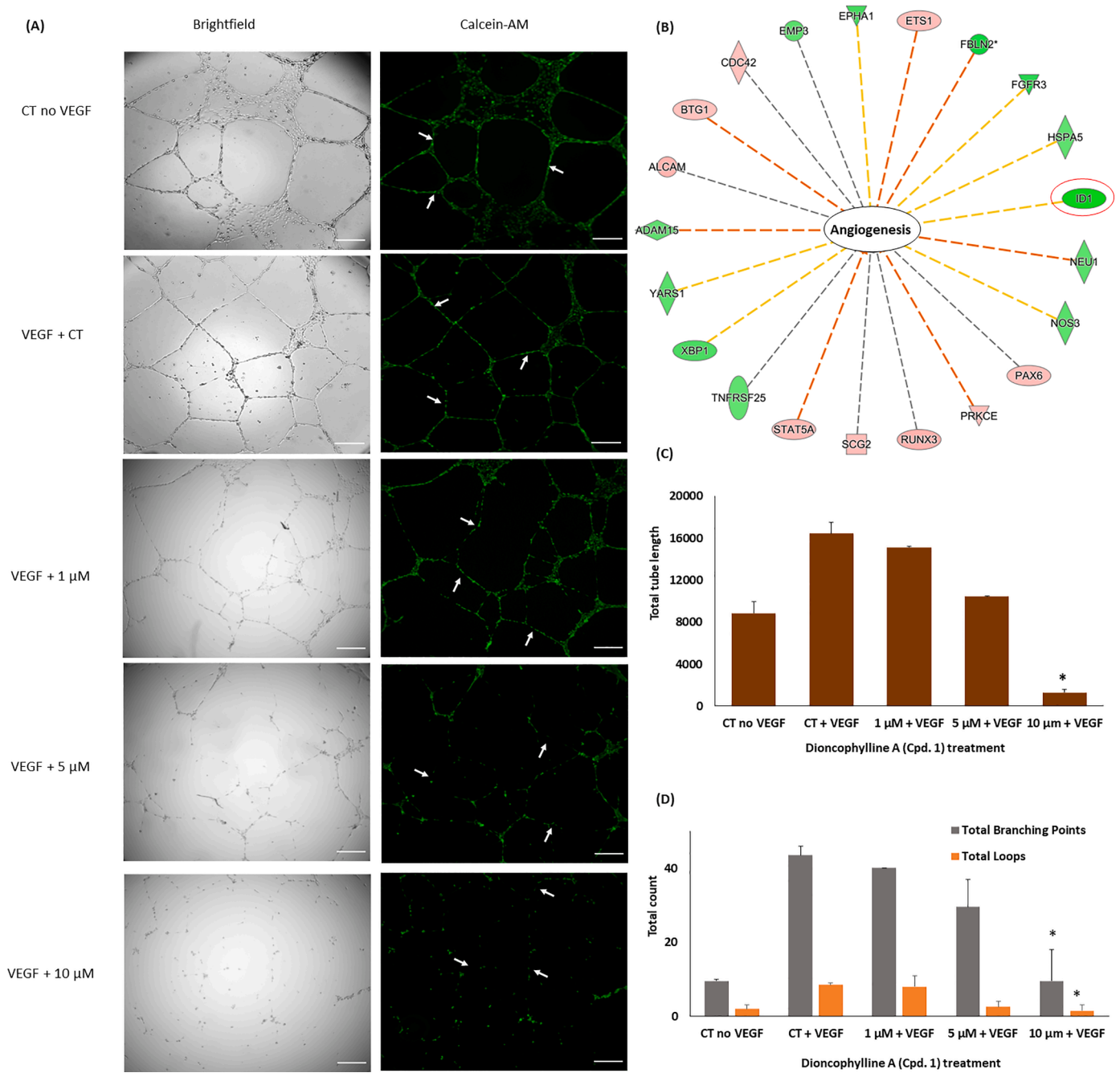

Fig. 8. Inhibition of tube formation by dioncophylline A. (A) Images of the cells that underwent the treatment with dioncophylline A in three different concentrations (1, 5, and 10 µM) after VEGF induction, the positive control DMSO with or without VEGF was also depicted. (B) Angiogenesis-associated molecules with dioncophylline A treatment predicted by IPA. Alterations in gene expression levels are illustrated using color codes: red indicates upregulation, while green signifies downregulation. (C and D) Suppression of total tube length and total branching points in HUVECs in a dose-dependent manner by dioncophylline A was shown indicating that dioncophylline A inhibited angiogenesis.

that were altered as a result of the treatment with RuT7 (Jovanović et al., 2016). To the best of our knowledge, this is the first report on microarray analyses of cell lines treated with dioncophylline A (Cpd. **1**). Since IPA analysis identified an NF-κB network as the top network, we addressed the question whether dioncophylline A or its derivatives bind to NF-κB *in silico* and inhibit it *in vitro*.

In silico studies predicted that dioncophylline A (Cpd. **1**) and two other ligands, Cpds. **2** and **3**, indeed bind to NF-κB and the binding site superimposed with that of triptolide (an NF-κB inhibitor). Then, the potentiality of the four NIQ ligands to inhibit the NF-κB pathway were tested using an NF-κB reporter assay. Not surprisingly, dioncophylline A showed the best inhibition effect on NF-κB activity. This finding motivated us to further explore the mode of cell death as well as the cellular function related to the NF-κB pathways such as cell cycle, and tube formation assay.

NF-κB as a transcription factor represents a critical modulator in inflammation and in tumor initiation, promotion, and progression (Barcellos-Hoff et al., 2013; Kaltschmidt et al., 2018). Its activation is involved in multiple hallmarks of cancer, including sustained proliferative signaling, evasion of growth suppressors, induction of angiogenesis, promotion of invasion and metastasis, and resistance to cell death (Taniguchi and Karin, 2018). NF-κB inhibition causes restraint of

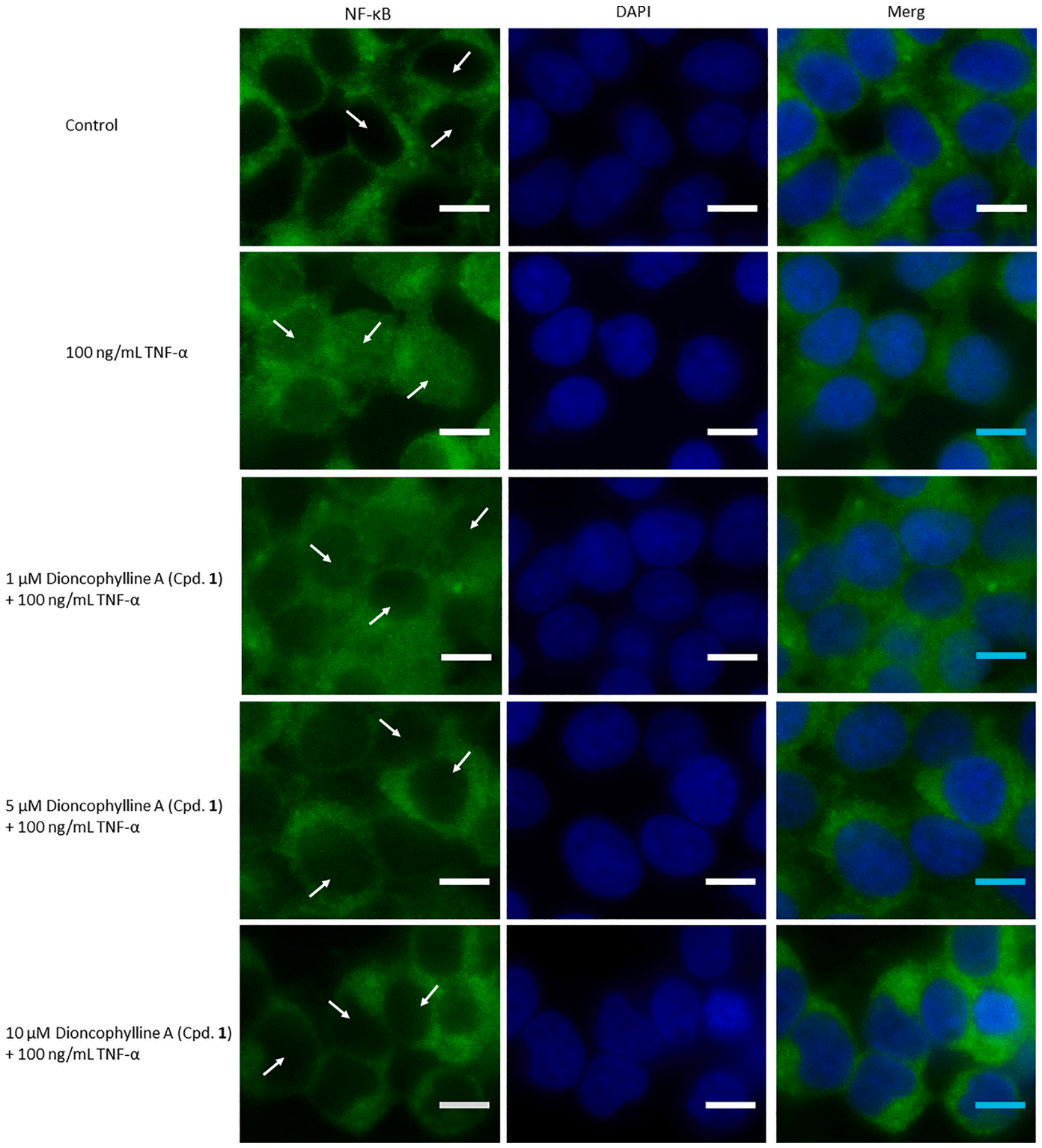

Fig. 9. Immunofluorescence visualizes the NF-κB translocation in HEK-Blue™ Null1 cells. TNF-α enhanced NF-κB translocation from the cytoplasm to the nucleus in the absence of dioncophylline A. However, TNF-α induced NK-κB translocation was inhibited by pre-treatment with dioncophylline A (1, 5, and 10 μM) for 24 h. An AF7000 widefield fluorescence microscope at 40 × magnification (scale bars = 10 μm) was used for visualization.

proliferation in fibroblast-like synovial cells and repression of arthritic angiogenesis (Xia et al., 2018b). If NF-κB was absent, autophagy was induced that is dependent on TNF-α through ROS accumulation and a swift increase in expression of Beclin 1, which is the central protein in autophagy and cell stress. Inhibition of autophagy was seen with NF-κB activation in various cancer cell lines including Ewing sarcoma, breast cancer, and promyelocytic leukemia (Djavaheri-Mergny et al., 2007, 2006; Verzella et al., 2020). Additionally, activation of NF-κB led to cell cycle alterations and to an induction of cell cycle arrest (Ledoux and Perkins, 2014).

Fluorescence microscopy provided evidence that dioncophylline A did not only inhibit the NF-κB pathway but also prevented its

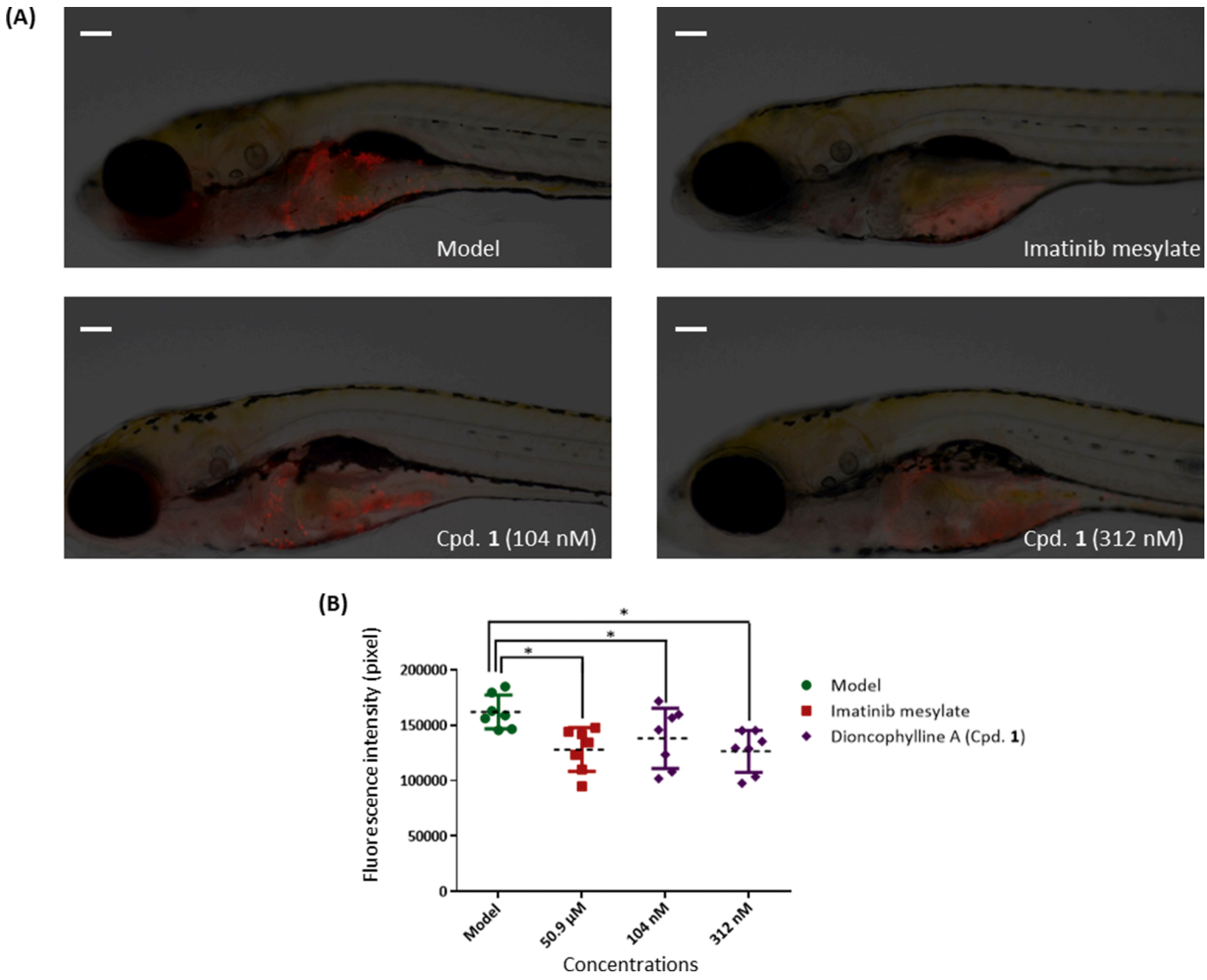

Fig. 10. The *in vivo* activity of dioncophylline A in a zebrafish model (A) The CCRF-CEM tumor mass is depicted by the red fluorescence. Images were captured at 60 × magnification (scale bars = 100 μm). (B) CCRF-CEM xenograft tumor zebrafish model showing fluorescence intensity and inhibition rate induced by dioncophylline A treatment for 48 h in two different concentrations (104 and 312 nM) compared to the positive control Imatinib mesylate. Compared to the negative control group, dioncophylline A intervention inhibited tumor growth and the effect dioncophylline A at 312 nM concentration is shown to be similar to the positive control. $^{*}p < 0.05$.

translocation from the cytoplasm to the nucleus. Mortier et al. (2010) reported that pyrazolo[4,3-*c*]isoquinolines inhibit TGF-β activated kinase 1 (TAK1), which is involved in the classical NF-κB pathway (Mortier et al., 2010). Many natural products are known to inhibit and modulate the NF-κB pathway. Isoprenoids, such as kaurene diterpenoids and members of the sesquiterpene lactones class such as parthenolide, phenolic compounds including curcumin and flavonoids such as silybin are known NF-κB modulators (Bremner and Heinrich, 2002). Moreover, some dimeric NIQ alkaloids such as michellamines exert anti-HIV effects (Lombe et al., 2019). As an example of dimeric benzylisoquinolines, cepharanthine suppress HIV-1 LTR driven gene expression through the inhibition of NF-κB activation (Okamoto et al., 1998).

DDIT4L, ETV5, LST1, ID1, and *SLC32A1* were the top-deregulated genes after treatment of CCRF-CEM with dioncophylline A (Cpd. **1**). The inhibitor of DNA binding 1 (*ID1*) participated in suppressed cellular processes upon dioncophylline A treatment such as the cell cycle. The ID proteins control cell cycle and cell differentiation. ID1 is most frequently associated with cancer, cellular senescence, and with cell proliferation and survival, out of all ID family proteins (Zhao et al., 2020).

A variety of cell death mechanisms have been identified and categorized according to cell shape, enzyme involvement, functional elements, and immunological traits (Kroemer et al., 2009). Here, we investigated both autophagy and apoptosis induction upon addition of dioncophylline A. Surprisingly, dioncophylline A did not extensively increase the number of apoptotic cells in comparison to the control sample, while it promoted autophagy similarly to rapamycin as assessed by flow cytometry. Recently, several groups also discovered that phytochemicals from Bulbine *frutescens* could induce apoptosis in breast cancer cells by changing the levels of procaspase. (Kushwaha et al., 2020b, 2019). Concerning autophagy, Awale et al. (2018) demonstrated for the first time that NIQ alkaloids such as ancistrolikokine E_3 are potent early-stage inhibitors of autophagy in human pancreatic cancer cells (Awale et al., 2018). Here, we found out that autophagy induction was achieved by dioncophylline A.

For the direct evaluation of cell cycle arrest induced by dioncophylline A, PI staining was carried out using flow cytometry. The treatment of CCRF-CEM with dioncophylline A resulted in an increased number of cells in G2/M arrest. Moreover, IPA analysis of the genes

deregulated by dioncophylline A revealed cell cycle progression as affected cellular functions. This finding is consistent with the fact that other plant-derived alkaloids such as paclitaxel, docetaxel, vinblastine, and vincristine are also known to induce cell cycle arrest (Badmus et al., 2019).

Angiogenesis is not only a vital process for normal tissue development. It is also largely associated with cancer, and its inhibition has important therapeutic effects. Therefore, an endothelial cell tube formation assay was developed to study angiogenesis *in vitro* (DeCicco-Skinner et al., 2014). One of the most interesting findings from IPA was the identification of angiogenesis as affected cellular functions, and the tube formation assay confirmed that dioncophylline A (Cpd. **1**) indeed inhibited angiogenesis. These results correspond to those of Hsu et al. (2022), who recently found that PPE8, a novel naphthoquinone-based compound also inhibited angiogenesis *in vitro* and *in vivo* via inhibition of micro vessel sprouting induced by VEGF-A (Hsu et al., 2022).

The zebrafish system is increasing in popularity as an *in vivo* model for the development of anti-cancer drugs and for the determination of toxicity (Konantz et al., 2013). Here, we used a zebrafish larvae CCRF-CEM cell xenograft model and demonstrated that dioncophylline A (Cpd. **1**) reduced tumor growth *in vivo*. Dioncophylline A did not show any abnormal phenotypes up to a concentration of 312 nM. It can be considered as an important result that dioncophylline A suppresses tumor growth *in vivo*. To the best of our knowledge, it is the first time to report the anti-cancer effect of NIQ alkaloids *in vivo* in general and of dioncophylline A in particular. Previous studies introduced zebrafish as a useful model to study tumor invasion, angiogenesis, metastasis, and carcinogenesis. Zebrafish larvae have a short reproductive cycle and no immunological rejection of human cells. They have a transparent body, which allows the visual monitoring of tumor development and treatment toxicity (Hill et al., 2018).

Conclusion

In conclusion, with the aim of developing a novel, highly efficient anticancer compound, we have introduced dioncophylline A (Cpd. **1**) as a potential anti-cancer candidate. Naphthylisoquinoline alkaloids have been proven to exert strong cytotoxicity towards leukemia cells. Moreover, this study for the first time provides insight into the mode of action of dioncophylline A in CCRF-CEM cells using microarray and IPA analyses. Dioncophylline A bound to NF-κB *in silico* and inhibited its translocation and significantly affected the NF-κB pathways *in vitro*. In addition, some other NIQs, Cpds. **2**–**4**, bound to NF-κB *in silico* and inhibited it *in vitro*. Several cell functions were impacted by dioncophylline A such as angiogenesis and cell cycle. On the other hand, dioncophylline A did not significantly induce apoptosis but autophagy instead, which may be the more relevant mode of cell death in this context. Remarkably, dioncophylline A also showed anti-tumor efficacy in zebrafish *in vivo*.

CRediT authorship contribution statement

Rümeysa Yücer: Methodology, Writing – original draft. **Shaimaa Fayez:** Methodology, Writing – original draft. **Doris Feineis:** Methodology. **Sabine M. Klauck:** Methodology, Writing – review & editing. **Letian Shan:** Methodology. **Gerhard Bringmann:** Investigation, Writing – review & editing, Validation. **Thomas Efferth:** Funding acquisition, Supervision, Writing – review & editing. **Mona Dawood:** Conceptualization, Methodology, Supervision, Writing – review & editing.

Declaration of competing interest

The authors declare that they have no known competing financial interests or personal relationships that could have appeared to influence the work reported in this paper.

Acknowledgments

We thank the Microarray Unit of the Genomics and Proteomics Core Facility, German Cancer Research Center (DKFZ) Heidelberg, for providing excellent Expression Profiling services.

Supplementary materials

Supplementary material associated with this article can be found, in the online version, at doi:10.1016/j.phymed.2023.155267.

References

Abdelfatah, S., Berg, A., Huang, Q., Yang, L., Hamdoun, S., Klinger, A., Greten, H.J., Fleischer, E., Berg, T., Wong, V.K.W., Efferth, T., 2019. MCC1019, a selective inhibitor of the Polo-box domain of Polo-like kinase 1 as novel, potent anticancer candidate. Acta Pharm. Sin. B 9, 1021–1034.

Abdelfatah, S., Nass, J., Knorz, C., Klauck, S.M., Kupper, J.H., Efferth, T., 2022. Pyrrolizidine alkaloids cause cell cycle and DNA damage repair defects as analyzed by transcriptomics in cytochrome P450 3A4-overexpressing HepG2 clone 9 cells. Cell Biol. Toxicol. 38, 325–345.

Awale, S., Dibwe, D.F., Balachandran, C., Fayez, S., Feineis, D., Lombe, B.K., Bringmann, G., 2018. Ancistrolikokine E_3, a 5,8′-coupled naphthylisoquinoline alkaloid, eliminates the tolerance of cancer cells to nutrition starvation by inhibition of the Akt/mTOR/autophagy signaling pathway. J. Nat. Prod. 81, 2282–2291.

Badmus, J.A., Ekpo, O.E., Hussein, A.A., Meyer, M., Hiss, D.C., 2019. Cytotoxic and cell cycle arrest properties of two steroidal alkaloids isolated from Holarrhena floribunda (G. Don) T. Durand & Schinz leaves. BMC Complem. Altern. M 19, 112.

Barcellos-Hoff, M.H., Lyden, D., Wang, T.C., 2013. The evolution of the cancer niche during multistage carcinogenesis. Nat. Rev. Cancer 13, 511–518.

Baud, V., Karin, M., 2009. Is NF-kappaB a good target for cancer therapy? Hopes and pitfalls. Nat. Rev. Drug Discov. 8, 33–40.

Bockers, M., Paul, N.W., Efferth, T., 2020. Bisphenolic compounds alter gene expression in MCF-7 cells through interaction with estrogen receptor alpha. Toxicol. Appl. Pharm. 399, 115030.

Bremner, P., Heinrich, M., 2002. Natural products as targeted modulators of the nuclear factor-kappa B pathway. J. Pharm. Pharmacol. 54, 453–472.

Bringmann, G., Holenz, J., Wiesen, B., Nugroho, B.W., Proksch, P., 1997. Dioncophylline A as a growth-retarding agent against the herbivorous insect *Spodoptera littoralis*: structure-activity relationships. J. Nat. Prod. 60, 342–347.

Bringmann, G., Jansen, J.R., Reuscher, H., Rübenacker, M., Peters, K., Von Schnering, H. G., 1990a. Acetogenic isoquinoline alkaloids. 17. First total synthesis of (-)-dioncophylline A (Triphyophylline) and of selected stereoisomers - complete (revised) stereostructure. Tetrahedron Lett. 31, 643–646.

Bringmann, G., Rübenacker, M., Jansen, J.R., Scheutzow, D., Aké Assi, L., 1990b. Acetogenic isoquinoline alkaloids.16. On the structure of the dioncophyllaceae alkaloids dioncophylline A (Triphyophylline) and O-methyl-triphyophylline. Tetrahedron Lett. 31, 639–642.

Bringmann, G., Zhang, G.L., Büttner, T., Bauckmann, G., Kupfer, T., Braunschweig, H., Brun, R., Mudogo, V., 2013. Jozimine A_2: the first dimeric dioncophyllaceae-type naphthylisoquinoline alkaloid, with three chiral axes and high antiplasmodial activity. Chem. -Eur. J. 19, 916–923.

Dawood, M., Fleischer, E., Klinger, A., Bringmann, G., Shan, L., Efferth, T., 2020a. Inhibition of cell migration and induction of apoptosis by a novel class II histone deacetylase inhibitor, MCC2344. Pharmacol. Res. 160, 105076.

Dawood, M., Hegazy, M.F., Elbadawi, M., Fleischer, E., Klinger, A., Bringmann, G., Kuntner, C., Shan, L., Efferth, T., 2020b. Vitamin K(3) chloro derivative (VKT-2) inhibits HDAC6, activates autophagy and apoptosis, and inhibits aggresome formation in hepatocellular carcinoma cells. Biochem. Pharmacol. 180, 114176.

Dawood, M., Ooko, E., Efferth, T., 2019a. Collateral sensitivity of parthenolide via NF-kappa B and HIF-alpha inhibition and epigenetic changes in drug-resistant cancer cell lines. Front. Pharmacol. 10.

Dawood, M., Ooko, E., Efferth, T., 2019b. Collateral sensitivity of parthenolide via NF-kappaB and HIF-alpha inhibition and epigenetic changes in drug-resistant cancer cell lines. Front. Pharmacol. 10, 542.

De Kouchkovsky, I., Abdul-Hay, M., 2016. Acute myeloid leukemia: a comprehensive review and 2016 update'. Blood Cancer J. 6, e441.

DeCicco-Skinner, K.L., Henry, G.H., Cataisson, C., Tabib, T., Gwilliam, J.C., Watson, N.J., Bullwinkle, E.M., Falkenburg, L., O'Neill, R.C., Morin, A., Wiest, J.S., 2014. Endothelial cell tube formation assay for the *in vitro* study of angiogenesis. J. Vis. Exp. e51312.

Djavaheri-Mergny, M., Amelotti, M., Mathieu, J., Besançon, F., Bauvy, C., Codogno, P., 2007. Regulation of autophagy by NF-kappaB transcription factor and reactives oxygen species. Autophagy 3, 390–392.

Djavaheri-Mergny, M., Amelotti, M., Mathieu, J., Besançon, F., Bauvy, C., Souquère, S., Pierron, G., Codogno, P., 2006. NF-κB activation represses tumor necrosis factor-α-induced autophagy. J. Biol. Chem. 281, 30373–30382.

Fayez, S., Cacciatore, A., Sun, S.J., Kim, M., Aké Assi, L., Feineis, D., Awale, S., Bringmann, G., 2021. Ancistrobrevidines A-C and related naphthylisoquinoline

alkaloids with cytotoxic activities against HeLa and pancreatic cancer cells, from the liana *Ancistrocladus abbreviatus*. Bioorgan Med. Chem. 30, 115950.
Fayez, S., Feineis, D., Aké Assi, L., Seo, E.J., Efferth, T., Bringmann, G., 2019. Ancistrobreveines A- D and related dehydrogenated naphthylisoquinoline alkaloids with antiproliferative activities against leukemia cells, from the West African liana *Ancistrocladus abbreviatus*. RSC Adv. 9, 15738–15748.
Fayez, S., Feineis, D., Mudogo, V., Seo, E.J., Efferth, T., Bringmann, G., 2018. Ancistrolikokine I and further 5,8′-coupled naphthylisoquinoline alkaloids from the Congolese liana *Ancistrocladus likoko* and their cytotoxic activities against drug-sensitive and multidrug resistant human leukemia cells. Fitoterapia 129, 114–125.
Feineis, D., Bringmann, G., 2023. Asian *Ancistrocladus* lianas as creative producers of naphthylisoquinoline alkaloids. In: Kinghorn, A.D., Falk, H., Gibbons, S., Asakawa, Y., Liu, J.-K., Dirsch, V.M. (Eds.), Progress in the Chemistry of Organic Natural Products. Springer International Publishing, Cham, Springer Nature Switzerland AG, Cham, Switzerland, pp. 1–335, 119.
François, G., Timperman, G., Eling, W., Aké Assi, L., Holenz, J., Bringmann, G., 1997. Naphthylisoquinoline alkaloids against malaria: evaluation of the curative potentials of dioncophylline C and dioncopeltine A against *Plasmodium berghei in vivo*. Antimicrob. Agents Ch. 41, 2533–2539.
Gillet, J.P., Efferth, T., Steinbach, D., Hamels, J., de Longueville, F., Bertholet, V., Remacle, J., 2004. Microarray-based detection of multidrug resistance in human tumor cells by expression profiling of ATP-binding cassette transporter genes. Cancer Res. 64, 8987–8993.
Hegazy, M.F., Fukaya, M., Dawood, M., Yan, G., Klinger, A., Fleischer, E., Zaglool, A.W., Efferth, T., 2020. Vitamin K_3 thio-derivative: a novel specific apoptotic inducer in the doxorubicin-sensitive and -resistant cancer cells. Invest. New Drugs 38, 650–661.
Hill, D., Chen, L., Snaar-Jagalska, E., Chaudhry, B., 2018. Embryonic zebrafish xenograft assay of human cancer metastasis. F1000Res 7, 1682.
Hsu, M.J., Chen, H.K., Lien, J.C., Huang, Y.H., Huang, S.W., 2022. Suppressing VEGF-A/VEGFR-2 signaling contributes to the anti-angiogenic effects of PPE8, a novel naphthoquinone-based compound. Cells-Basel 11.
Hwang, D., Kim, M., Park, H., Jeong, M.I., Jung, W., Kim, B., 2019. Natural products and acute myeloid leukemia: a review highlighting mechanisms of action. Nutrients 11.
Jovanović, K.K., Tanic, M., Ivanovic, I., Gligorijevic, N., Dojcinovic, B.P., Radulovic, S., 2016. Cell cycle, apoptosis, cellular uptake and whole-transcriptome microarray gene expression analysis of HeLa cells treated with a ruthenium(II)-arene complex with an isoquinoline-3-carboxylic acid ligand. J. Inorg. Biochem. 163, 362–373.
Kadioglu, O., Saeed, M., Greten, H.J., Efferth, T., 2021. Identification of novel compounds against three targets of SARS CoV-2 coronavirus by combined virtual screening and supervised machine learning. Comput. Biol. Med. 133.
Kaltschmidt, B., Greiner, J.F.W., Kadhim, H.M., Kaltschmidt, C., 2018. Subunit-specific role of NF-κB in cancer. Biomedicines 6, 44.
Konantz, M., Paczulla, A., Grzywna, S., Kanz, L., Lengerke, C., 2013. Zebrafish xenografts as a tool for *in vivo* studies on human cancer. Onkologie 36, 275–276.
Kroemer, G., Galluzzi, L., Vandenabeele, P., Abrams, J., Alnemri, E.S., Baehrecke, E.H., Blagosklonny, M.V., El-Deiry, W.S., Golstein, P., Green, D.R., Hengartner, M., Knight, R.A., Kumar, S., Lipton, S.A., Malorni, W., Nunez, G., Peter, M.E., Tschopp, J., Yuan, J., Piacentini, M., Zhivotovsky, B., Melino, G., Nomenclature Committee on Cell, D., 2009. Classification of cell death: recommendations of the nomenclature committee on cell death 2009. Cell Death Differ. 16, 3–11.
Kuete, V., Efferth, T., 2013. Molecular determinants of cancer cell sensitivity and resistance towards the sesquiterpene farnesol. Pharmazie 68, 608–615.
Kushwaha, P.P., Singh, A.K., Prajapati, K.S., Shuaib, M., Fayez, S., Bringmann, G., Kumar, S., 2020a. Induction of apoptosis in breast cancer cells by naphthylisoquinoline alkaloids. Toxicol. Appl. Pharmacol. 409, 115297.
Kushwaha, P.P., Singh, A.K., Shuaib, M., Prajapati, K.S., Vardhan, P.S., Gupta, S., Kumar, S., 2020b. 3-O-(E)-p-Coumaroyl betulinic acid possess anticancer activity and inhibit Notch signaling pathway in breast cancer cells and mammosphere. Chem. -Biol. Interact. 328.
Kushwaha, P.P., Vardhan, P.S., Kapewangolo, P., Shuaib, M., Prajapati, S.K., Singh, A.K., Kumar, S., 2019. Bulbine frutescens phytochemical inhibits notch signaling pathway and induces apoptosis in triple negative and luminal breast cancer cells. Life Sci. 234, 116783.
Ledoux, A.C., Perkins, N.D., 2014. NF-κB and the cell cycle. Biochem. Soc. Trans. 42, 76–81.
Li, J., Seupel, R., Bruhn, T., Feineis, D., Kaiser, M., Brun, R., Mudogo, V., Awale, S., Bringmann, G., 2017a. Jozilebomines A and B, naphthylisoquinoline dimers from the congolese liana *Ancistrocladus ileboensis*, with antiausterity activities against the PANC-1 human pancreatic cancer cell line. J. Nat. Prod. 80, 2807–2817.
Li, J., Seupel, R., Feineis, D., Mudogo, V., Kaiser, M., Brun, R., Brunnert, D., Chatterjee, M., Seo, E.J., Efferth, T., Bringmann, G., 2017b. Dioncophyllines C_2, D_2, and F and related naphthylisoquinoline alkaloids from the congolese liana *Ancistrocladus ileboensis* with potent activities against *Plasmodium falciparum* and against multiple myeloma and leukemia cell lines. J. Nat. Prod. 80, 443–458.
Li, W., Liang, J., Zhang, Z., Lou, H., Zhao, L., Xu, Y., Ou, R., 2017c. MicroRNA-329-3p targets MAPK1 to suppress cell proliferation, migration and invasion in cervical cancer. Oncol. Rep. 37, 2743–2750.
Lin, A., Karin, M., 2003. NF-kappaB in cancer: a marked target. Semin. Cancer Biol. 13, 107–114.
Livak, K.J., Schmittgen, T.D., 2001. Analysis of relative gene expression data using real-time quantitative PCR and the 2(T)(-Delta Delta C) method. Methods 25, 402–408.
Lombe, B.K., Bruhn, T., Feineis, D., Mudogo, V., Brun, R., Bringmann, G., 2017. Antiprotozoal spirombandakamines A_1 and A_2, fused naphthylisoquinoline dimers from a congolese *Ancistrocladus* plant. Org. Lett. 19, 6740–6743.
Lombe, B.K., Feineis, D., Bringmann, G., 2019. Dimeric naphthylisoquinoline alkaloids: polyketide-derived axially chiral bioactive quateraryls. Nat. Prod. Rep. 36, 1513–1545.
Mahmoud, N., Dawood, M., Huang, Q., Ng, J.P.L., Ren, F., Wong, V.K.W., Efferth, T., 2022. Nimbolide inhibits 2D and 3D prostate cancer cells migration, affects microtubules and angiogenesis and suppresses B-RAF/p.ERK-mediated *in vivo* tumor growth. Phytomed.: Int. J. Phytother. Phytopharmacol. 94, 153826.
Mahmoud, N., Saeed, M.E.M., Sugimoto, Y., Klauck, S.M., Greten, H.J., Efferth, T., 2018. Cytotoxicity of nimbolide towards multidrug-resistant tumor cells and hypersensitivity via cellular metabolic modulation. Oncotarget 9, 35762–35779.
Martin, T.A., Ye, L., Sanders, A.J., Lane, J., Jiang, W.G., 2013. Cancer Invasion and metastasis: Molecular and Cellular perspective, Madame Curie Bioscience Database [Internet]. Landes Bioscience.
Mortier, J., Frederick, R., Ganeff, C., Remouchamps, C., Talaga, P., Pochet, L., Wouters, J., Piette, J., Dejardin, E., Masereel, B., 2010. Pyrazolo[4,3-c]isoquinolines as potential inhibitors of NF-kappa B activation. Biochem. Pharmacol. 79, 1462–1472.
Moyo, P., Shamburger, W., van der Watt, M.E., Reader, J., de Sousa, A.C.C., Egan, T.J., Maharaj, V.J., Bringmann, G., Birkholtz, L.M., 2020. Naphthylisoquinoline alkaloids, validated as hit multistage antiplasmodial natural products. Int J Parasitol-Drug 13, 51–58.
O'Brien, J., Wilson, I., Orton, T., Pognan, F., 2000. Investigation of the Alamar Blue (resazurin) fluorescent dye for the assessment of mammalian cell cytotoxicity. Eur. J. Biochem. 267, 5421–5426.
Okamoto, M., Ono, M., Baba, M., 1998. Potent inhibition of HIV type 1 replication by an antiinflammatory alkaloid, cepharanthine, in chronically infected monocytic cells. AIDS Res. Hum. Retroviruses 14, 1239–1245.
Ponte-Sucre, A., Faber, J.H., Gulder, T., Kajahn, I., Pedersen, S.E., Schultheis, M., Bringmann, G., Moll, H., 2007. Activities of naphthylisoquinoline alkaloids and synthetic analogs against *Leishmania major*. Antimicrob. Agents Chemother. 51, 188–194.
Saeed, M.E., Mahmoud, N., Sugimoto, Y., Efferth, T., Abdel-Aziz, H., 2018. Molecular determinants of sensitivity or resistance of cancer cells toward sanguinarine. Front. Pharmacol. 9, 136.
Tajuddeen, N., Bringmann, G., 2021. N,C-Coupled naphthylisoquinoline alkaloids: a versatile new class of axially chiral natural products. Nat. Prod. Rep. 38, 2154–2186.
Tajuddeen, N., Van Heerden, F.R., 2019. Antiplasmodial natural products: an update. Malaria J. 18, 404.
Tallman, M.S., Gilliland, D.G., Rowe, J.M., 2005. Drug therapy for acute myeloid leukemia. Blood 106, 1154–1163.
Taniguchi, K., Karin, M., 2018. NF-κB, inflammation, immunity and cancer: coming of age. Nat. Rev. Immunol. 18, 309–324.
Trask, O.J., Jr., 2004. Nuclear factor kappa B (NF-kappaB) translocation assay development and validation for high content screening, in: Markossian, S., Grossman, A., Brimacombe, K., Arkin, M., Auld, D., Austin, C. et al. (Eds.), Assay Guidance Manual, Bethesda (MD).
Tshitenge, D.T., Feineis, D., Mudogo, V., Kaiser, M., Brun, R., Seo, E.J., Efferth, T., Bringmann, G., 2018. Mbandakamine-type naphthylisoquinoline dimers and related alkaloids from the Central African Liana *Ancistrocladus ealaensis* with antiparasitic and antileukemic activities. J. Nat. Prod. 81, 918–933.
Verzella, D., Pescatore, A., Capece, D., Vecchiotti, D., Ursini, M.V., Franzoso, G., Alesse, E., Zazzeroni, F., 2020. Life, death, and autophagy in cancer: nF-κB turns up everywhere. Cell Death. Dis. 11, 210.
Xia, L., Tan, S., Zhou, Y., Lin, J., Wang, H., Oyang, L., Tian, Y., Liu, L., Su, M., Wang, H., Cao, D., Liao, Q., 2018a. Role of the NFkappaB-signaling pathway in cancer. Oncol. Targets Ther. 11, 2063–2073.
Xia, Y.F., Shen, S., Verma, I.M., 2014. NF-kappa B, an active player in human cancers. Cancer Immunol. Res. 2, 823–830.
Xia, Z.B., Meng, F.R., Fang, Y.X., Wu, X., Zhang, C.W., Liu, Y., Liu, D., Li, G.Q., Feng, F.B., Qiu, H.Y., 2018b. Inhibition of NF-κB signaling pathway induces apoptosis and suppresses proliferation and angiogenesis of human fibroblast-like synovial cells in rheumatoid arthritis. Medicine (Baltimore). 97, e10920.
Zhao, Z., Bo, Z., Gong, W., Guo, Y., 2020. Inhibitor of differentiation 1 (Id1) in cancer and cancer therapy. Int. J. Med. Sci. 17, 995–1005.